ANALIZA PERFORMANSI OŠTEĆENIH OBJEKATA, PRIMENOM SCENARIJA POVEZANIH NELINEARNIH ANALIZA I KOEFICIJENTA OŠTEĆENJA

PERFORMANCE ANALYSIS OF DAMAGED BUILDINGS APPLYING SCENARIO OF RELATED NON-LINEAR ANALYSES AND DAMAGE COEFFICIENT

Mladen ĆOSIĆ
Radomir FOLIĆ

ORIGINALNI NAUČNI RAD
ORIGINAL SCIENTIFIC PAPER
UDK: 699.844:550.344
doi: 10.5937/grmk1503003C

1 UVOD

Analiza stanja oštećenih objekata predstavalja kompleksan inženjerski problem i zahteva anagažovanje eksperata, tj. inženjera s višegodišnjim iskustvom u proceni stanja objekata. U praksi, početna procena oštećenja objekata najčešće se bazira na empiriji, uz kvalitativan opis stanja objekta, a zatim i kvantitativnoj primeni linearnih numeričkih modela i dimenzionisanja prema propisima. S druge strane, razvoj savremenih softvera za nelinearnu analizu konstrukcija i metodologije projektovanja konstrukcija prema seizmičkim performansama (PBSD) otvara mogućnost za pouzdaniji i multiparametarski pristup u proceni stanja objekata. Generalno razmatrajući, procenu nivoa oštećenja objekata moguće je sprovesti primenom: simplifikovanih analiza, analitičkih procedura, energetskih kriterijuma, indeksa oštećenja, proračuna performansi sistema plastičnom analizom (PBPD), krivih osetljivosti, numeričkih jednokoračnih analiza, inkrementalno-iterativnih analiza, nelinearne statičke *pushover* analize (NSPA), nelinearne dinamičke analize (NDA) i inkrementalne nelinearne dinamičke analize (INDA).

Jedan od najčešće korišćenih parametara u oceni stepena oštećenja objekata, za dejstvo zemljotresa, jeste globalni indeks oštećenja [33], [15]. Indikatori oštećenja su nekumulativni, kumulativni i kombinovani. Parametri odgovora koji se koriste za proračun indikatora oštećenja jesu: nivo maksimalnih deformacija sistema, histerezisno ponašanje i apsorpcija energije.

Dr Mladen Ćosić, nezavisni istraživač, Marka Milanovića 17, 15300 Loznica, mladen.cosic@ymail.com
Profesor emeritus dr Radomir Folić, Univerzitet u Novom Sadu, Fakultet tehničkih nauka, Trg Dositeja Obradovića 6, 21000 Novi Sad folic@uns.ac.rs

1 INTRODUCTION

The complex engineering problem of analyzing the conditions/state of damaged buildings requires experts i.e. engineers with huge experience in assessing the state of buildings. In practice, the initial assessment of damage to structures is usually empirically-based with a qualitative description of their state, followed by a quantitative description using linear numerical models and dimensioning according to the regulations. However, the latest non-linear structural analysis software and the emerging designing methodologies using *Performance-Based Seismic Design* (PBSD), indicate the possibility for reliable and multi-parameter approach in assessing the state of the structure. Generally, the level of damage to structures can be assessed based on the following: simplified analysis, analytical procedures, energy criteria, damage index, calculating system performance using *Performance-Based Plastic Design* (PBPD), fragility curves, numerical one step solution, incremental-iterative analysis, *Non-linear Static Pushover Analysis* (NSPA), *Non-linear Dynamic Analysis* (NDA) and *Incremental Non-linear Dynamic Analysis* (INDA).

One of the most common parameters used in assessing structural damage levels induced by earthquake action is the global damage index [33] and [15]. Damage indicators can be non-cumulative, cumulative and combined. Response parameters used for calculating the damage indicators are the following: maximum system deformation level, hysteresis behaviour and energy

Dr Mladen Ćosić, independent scientist, Marka Milanovića 17, 15300 Loznica, mladen.cosic@ymail.com
Professor emeritus Dr Radomir Folić, University of Novi Sad, Faculty of Technical Sciences, Trg Dositeja Obradovića 6, 21000 Novi Sad folic@uns.ac.rs

Globalni indeksi oštećenja jesu: prosečni težinski indeksi [28], [29], [5] i indeksi određeni na osnovu modalnih parametara [30], [7]. Unapređeni indeks oštećenja 2D modela zgrada prikazan je u [20], dok je u [19] prikazan indeks oštećenja za 3D modele zgrada. Procena nivoa oštećenja zgrada, na osnovu rezidualnog seizmičkog kapaciteta, razmatrana je u radu [25]. Klase oštećenja usvojene su prema [27]: prvi nivo oštećenja - počev od iniciranja prslina do pojave napona tečenja u šipkama armature; drugi i treći nivo oštećenja do iniciranja loma pri pritisku u betonu; četvrti nivo do izvijanja podužnih šipki armature i odlamanja zaštitnog sloja betona; peti nivo - do potpunog kolapsa konstrukcije. Istraživanje na temu kontrolisanog mehanizma loma sistema, proračunom prema silama (FBD), prezentovano je u [26]. Primenom energetskog koncepta i metode spektra odgovora za nivo granice tečenja (YPS), razmatrane su funkcije oštećenja zgrada preko: faktora modifikacije pomeranja, faktora redukcije nosivosti na granici tečenja, parametra seizmičke energije, indeksa oštećenja, koeficijenta ekvivalentne duktilnosti [24]. Razmatranje mogućnosti razvoja različitih mehanizama loma okvirnih sistema zgrada (MRF) - od spratnog do kombinovanog - prikazano je u radu [31], dok je u radovima [1], [2] izvršena identifikacija kolapsnog mehanizma loma sistema na osnovu spektra kapaciteta kolapsa. Generalna podela razvoja mehanizma loma sistema jeste na lokalni i gobalni. U radu [22] prikazani su primeri zgrada gde su, usled dejstva zemljotresa, razvijeni spratni (lokalni) mehanizmi loma s potpunim kolapsom i bez njega. Takođe, ukazano je i na formiranje mehanizma loma po svim spratovima (globalnog), bez potpunog kolapsa zgrade. U istraživanju [32], iniciranje mehanizma kolapsa zgrada i globalne dinamičke nestabilnosti sistema razmatrano je u funkciji međuspratnog drifta i spektralnih akceleracija primenom inkrementalne dinamičke analize (IDA). Takođe, mnogi rezultati istraživanja na temu mehanizama oštećenja i loma zgrada IDA analizom u kapacitativnom domenu prikazani su u [4], [16], [17], [21].

U ovom radu predstavljena je procedura kojom se simulacijom - putem scenarija međusobno povezanih analiza - doprinosi uvidu o stanju, a koja je važna za odluku o neophodnim intervencijama ili uklanjanju to jest rušenju konstrukcije. Na primeru armiranobetonske zgrade s deset etaža, prikazana je razvijena procedura kojom se u incidentnoj situaciji utvrđuje adaptabilnost sistema, koji je i dodatno izložen dejstvu zemljotresa. S obzirom na to što se prema PBSD metodologiji razmatraju performanse sistema, primenom nelinearnih numeričkih modela, dovodeći ga do stanja pretkolapsa, odnosno kolapsa, to se primenom ovako razvijene procedure mogu pouzdano donositi odluke o stanju zgrade.

2 SCENARIO POVEZANIH NELINEARNIH ANALIZA

Koncept scenarija povezanih nelinearnih analiza, razvijen i prikazan u ovom istraživanju i u [14], zasniva se na utvrđivanju stanja objekta, uvažavajući principe projektovanja konstrukcija prema seizmičkim performansama (PBSD). Klasičan pristup u proceni stanja oštećenog objekta polazi od nedestruktivnih metoda, uzimanja uzoraka, empirijskim procenama i proračunom objekata primenom linearnih analiza.

absorption. Global damage indices include average weight indices [28], [29], [5] and indices identified based on modal parameters [30] and [7]. The improved damage index for 2D building models is presented in [20], while [19] discusses the damage index for 3D models. The assessment of damage levels to buildings based on the residual seismic capacity is discussed in [25]. Damage classes have been adopted according to [27]: the first level of damage between cracks initiation and appearance of yield in reinforcement bars, the second and third level of damage before the initiation of pressure-induced concrete fracture, the fourth level before the buckling of longitudinal reinforcement bars and spalling off of the protective concrete layer, and the fifth level up to the collapse of the building. The research regarding the system's controlled fracture mechanism using the *Force-Based Design* (FBD) is presented in [26]. Applying the energy concept and the *Yield Point Spectra Method* the structures' damage functions were considered using: the displacement modification factor, yield strength reduction factor, seismic energy response parameter, damage index and equivalent ductility ratio [24]. Possibilities of developing various fracture mechanisms in the moment resisting frame (MRF), both in storey and combined levels, are shown in [31], while in [1] and [2] the collapse mechanism of system fracture are identified on the basis of collapse capacity spectra. Generally, the system's fracture mechanism can develop locally or globally. In [22] examples of buildings are presented where earthquake-induced storey-level (local) fracture mechanisms occurred with and without a total collapse. The formation of fracture mechanism along all storeys (global) without the building's total collapse is also indicated. Initiation of the collapse mechanism and the system's global dynamic instability were discussed in [32] as a function of inter-storey drifts and spectral acceleration using the IDA analysis. A number of results on damage and fracture mechanisms obtained using IDA analysis in capacitive domain are presented in [4], [16], [17] and [21].

This paper describes a procedure of simulating the scenarios of interrelated analyses, providing thereby a better insight in the state of the building and facilitating decisions on necessary interventions or the removal/demolition of the building. On the example of a ten storey reinforced concrete building, a procedure has been developed for determining the adaptability in accidental situations of the system additionally exposed to earthquake actions. Given the fact that the PBSD methodology requires system performance to be considered using non-linear numerical models bringing the system into a pre-collapse or collapse state, these advanced procedures enable the aforementioned decisions about the building to be highly reliable.

2 SCENARIO OF RELATED NON-LINEAR ANALYSES

The concept of the scenario of related non-linear analyses, presented in this research and in [14], is based on determining the structural condition while observing the *Performance-Based Seismic Design* (PBSD) principles. The classical approach in the assessment of a damaged structure starts from the non-destructive methods, sample taking, empirical

Proračun graničnih stanja nosivosti i upotrebljivosti sprovodi se prema propisima, pri čemu prednost treba dati modernim evropskim propisima EN 1992 [8] i EN 1998 [9]. Međutim, ovi propisi ne definišu detaljno oblasti u kojima se razmatraju objekti koji su u toku svog eksploatacionog veka oštećeni incidentnim dejstvima, kao što je dejstvo projektila (objekti bombardovani u Srbiji 1999. godine), nagli kolaps jednog ili nekoliko konstruktivnih elemenata i slične incidentne situacije. Takođe, znatan broj objekata nakon dejstva snažnog zemljotresa ne sanira se u predviđenom periodu, pa budu izloženi ili naknadnim zemljotresima manjih intenziteta ili afteršokovima koji mogu dodatno ugroziti nosivost, stabilnosti i upotrebljivost već oštećenog objekta [23]. Slična situacija je i sa objektima koji su bombardovani u Srbiji 1999. godine. Neki od ovih objekata i do danas nisu sanirani, tako da u postojećem oštećenom obliku dodatno predstavljaju opasnost za korisnike ili prolaznike koji se kreću u njihovoj neposrednoj blizini.

Aspekti na koje ukazuju evropski propisi pri proračunu oštećenih objekata uglavnom se odnose na primenu linearnih statičkih analiza i dimenzionisanja armiranobetonskih elemenata. Procedure koje definišu nelinearne analize objekata svedene su na minimum. U odnosu na evropske propise, američki propisi FEMA 273 [11], FEMA 274 [12] i FEMA 356 [13] detaljnije razmatraju procene stanja i sanacije objekata koji su izloženi dejstvu zemljotresa. Međutim, ne uzimaju se u obzir druga incidentna dejstva i povezanost numeričkih modela pre i posle oštećenja. S ciljem jasnijeg definisanja i tačnijeg proračuna ovako složenog problema, razvijen je scenario povezanih nelinearnih analiza, koji je potrebno sprovesti kako bi se mogle doneti kvalitetne odluke o stanju objekta. Na slici 1 prikazan je dijagram toka scenarija povezanih nelinearnih analiza. U prvom delu sprovodi se proračun, primenom linearne statičke analize (LSA) i spektralne-modalne analize (SMA). Zatim, dimenzionisanjem prema EN 1992 [8] i EN 1998 [9] propisima određuje se potrebna armatura u armiranobetonskim presecima. U drugom delu se kreira nov 3D model objekta za nelinearne analize. U prvom koraku drugog dela proračunavaju se statički uticaju u presecima objekata samo za vertikalna gravitaciona dejstva (stalno, korisno i slična opterećenja). Matrica krutosti sistema na kraju ove analize koristi se kao inicijalna matrica krutosti prilikom nelinearne statičke *pushover* analize (NSPA) za bidirekciono seizmičko dejstvo (X i Y pravac), koja se sprovodi u drugom koraku drugog dela. Kao nelinearni odgovor sistema, dobijaju se *pushover* krive, ciljno pomeranje, sile i momenti u presecima, globalni (*DR*) i međuspratni driftovi (*IDR*). U trećem delu sprovodi se simulacija incidentnog dejstva na konstrukciji, pri čemu nastupa oštećenje objekta redukcijom nosivosti, stabilnosti i upotrebljivosti pojedinih stubova. Matrica krutosti sistema prethodne analize koristi se kao inicijalna matrica krutosti nelinearne analize (NA - *Nonlinear Analysis*) kojom se simulira oštećenje objekta. Matematička formulacija analize incidentnog dejstva izvedena je polazeći od izraza za stanje neoštećenog objekta:

assessment and design of structures using linear analyses. The ultimate limit state and service life calculations are conducted according to the regulations, with contemporary European codes EN 1992 [8] and EN 1998 [9] being primary. However, these codes fail to define in detail the areas in which the buildings are considered, which were damaged during their service life by accidental action, such as the effects of the projectiles (structures in Serbia bombed in 1999), sudden collapse of one or several structural elements and similar accidental situations. Also, a significant number of buildings upon the impact of a strong earthquake are unrepaired within the prescribed period and thus exposed to either subsequent earthquakes of smaller intensity or aftershocks which can be further impair of the bearing capacity, stability and usability on the already damaged building [23]. The situation is similar with buildings that were bombed in Serbia in 1999. A number of these structures are still unrepaired, and thus, their existing damaged state additionally endangers their users or pedestrians in their immediate vicinity.

Aspects indicated by the European regulations listed in the calculation of damaged buildings are mostly related to the use of linear static analyses and dimensioning reinforced concrete elements. The procedures defining the non-linear analyses of structures are minimized. In comparison to the European regulations, the American regulations FEMA 273 [11], FEMA 274 [12] and FEMA 356 [13] consider the assessments of conditions and rehabilitation of the structures, which were exposed to earthquake action in detail. However, they fail to take into consideration other accidental actions and relatedness of numerical models before and after sustaining damage. For the purpose of clearer defining and more accurate calculation of such complex problem, the scenario of related non-linear analyses is developed, which must be performed in order to make adequate decisions on the condition of the structure. A flow chart of scenarios of the related non-linear analyses is presented in Figure 1. In the first part, the calculation is conducted implementing the *Linear Static Analysis* (LSA) and *Spectral - Modal Analysis* (SMA). Further, by designing in compliance with EN 1992 [8] and EN 1998 [9] codes, the necessary reinforcement in RC cross-sections is determined. In the second part a new 3D model of building is created for the non-linear analysis. At the first step of the second part, the static effects in the cross-sections of the structures are calculated only for vertical gravity actions (dead, super dead, live and similar loads). At the end of this analysis the system stiffness matrix is used as the initial stiffness matrix in the *Non-linear Static Pushover Analysis* (NSPA) for bidirectional seismic action (X and Y directions), which is conducted in the second step of the second part. As a non-linear response of the system the pushover curves, target displacement, forces and moments in cross sections, global drift (*DR*) and inter-storey drifts (*IDR*) are obtained. In the third part, the simulation of accidental action on the structure is conducted, so the action causing decreases of bearing capacity, stability and serviceability of individual columns. The system stiffness matrix of the previous analysis is used as initial stiffness matrix of the non-linear analysis (NA) which simulates structural damage.

The mathematical formulation for analyzing accidental action is derived based on the expression for the state of the undamaged building:

$$[K_0]\{D_0\} = \{P_0\}, \tag{1}$$

gde je [K_0] matrica krutosti neoštećenog objekta, {D_0} vektor pomeranja neoštećenog objekta i {P_0} vektor opterećenja neoštećenog objekta. Za *i*-ti scenario oštećenja analiza se sprovodi prema:

where [K_0] is the stiffness matrix of the undamaged building, {D_0} is the displacement vector of the undamaged building and {P_0} is the load vector of the undamaged building. For the *i*-th damage scenario, the analysis is conducted based on:

$$[K_i]\{D_i\} = \{P_i\}, \quad [K_i] = [K_0] - [K_i'], \quad [M_i] = [M_0] - [M_i'], \tag{2}$$

gde je [K_i] matrica krutosti oštećenog objekta, {D_i} vektor pomeranja oštećenog objekta, {P_i} vektor opterećenja oštećenog objekta, $[K_i']$ matrica krutosti eliminisanih stubova, [M_i] matrica masa oštećenog objekta, [M_0] matrica masa neoštećenog objekta i $[M_i']$ matrica masa eliminisanih stubova.

U ovom slučaju može se pratiti razvoj nelinearnih deformacija i preraspodela statičkih uticaja u sistemu. Posebno je interesantno to što se ovakvom analizom može sprovoditi monitoring plastičnih defomacija u zoni jako oštećenih stubova, odnosno monitoring razvoja plastičnih zglobova na gredama koje su pozicionirane u zoni lokalnog kolapsa. Broj mogućih scenarija *n* oštećenja objekta i kolapsa pojedinih stubova može biti znatan. U četvrtom delu matrica krutosti sistema na kraju analize oštećenja objekta koristi se kao inicijalna matrica krutosti NSPA analize za bidirekciono seizmičko dejstvo (X i Y pravac), pri čemu se kao nelinearni odgovori sistema dobijaju *pushover* krive, ciljno pomeranje, sile i momenti u presecima, globalni *DR* i međuspratni *IDR* driftovi. U petom delu se proračunava koeficijent oštećenja C_d za svaki scenario i seizmičko dejstvo (X i Y pravac) pojedinačno. Po završetku proračuna objekta po svim predefinisanim scenarijima, a na osnovu proračunatih *pushover* krivih, globalnih *DR* i međuspratnih *IDR* driftova, formiranih mehanizama loma sistema i koeficijenata oštećenja C_d, utvrđuje se da li je potrebno objekat sanirati, pojačati ili delimično promeniti statički sistem u zoni kolapsa stubova. Ukoliko je potrebno sprovesti neki od predloženih postupaka, tada se redimenzioniše objekat i eventualno ponavlja procedura radi verifikacije i komparacije dobijenih rešenja. Kao što se može primetiti, ovako koncipiranim proračunom oštećenog objekta simulira se realistično ponašanje u uslovima dejstva i incidentne situacije i seizmičkog dejstva, budući da se prvo objekat izloži dejstvu gravitacionog opterećenja, a zatim se ovako opterećena konstrukcija izlaže incidentnom dejstvu. Nakon toga, povredljivost objekta proverava se na deformisanom i oštećenom objektu, dok se kroz sve proračune gravitaciono opterećenje samo prenosi iz početne u naredne analize, a incidentno i seizmičko dejstvo se definiše u njima odgovarajućim analizama.

Tekst uz sl. 1 nije preveden na srpski jezik jer je obrazložen u tekstu.

where [K_i] is the stiffness matrix of the damaged building, {D_i} is the displacement vector of the damaged building, {P_i} is the load vector of the damaged building, $[K_i']$ is the stiffness matrix of eliminated columns, [M_i] is the mass matrix of the damaged building, [M_0] is the mass matrix of the undamaged building and $[M_i']$ is the mass matrix of eliminated columns.

In this case, development of non-linear strains in the system can be monitored, as well as the redistribution of static influences in the system. It is of particular importance that such analysis can serve for monitoring plastic strain in the zone of severely damaged columns, i.e. monitoring development of plastic hinges on the beams that are located in the local collapse zone. The number of possible scenarios *n* of structural damage and collapse of individual columns can be considerable. In the fourth part, the system stiffness matrix at the end of the structural damage analysis is used as initial stiffness matrix of NSPA analysis for bidirectional seismic action (X and Y direction), whereby the pushover curves are obtained as non-linear responses of the system, as well as target displacement, forces and moments in cross-sections, global *DR* and inter-storey drifts *IDR*. In the fifth section, the damage coefficient C_d has been calculated for each scenario and seismic action (X and Y directions) individually. Decisions regarding the possible need for repairing, reinforcing or partially changing the static system of the building in the zone of collapsed columns are made based on calculated pushover curves, global *DR* and inter-storey *IDR* drifts, established fracture mechanisms and damage coefficient C_d upon the completion of the calculation on all pre-defined scenarios. If it is necessary to conduct some of the proposed procedures, the structure is redesigned, and possibly the procedure is reiterated for the purpose of verification and comparison of the obtained solutions. As it can be noticed, the calculation of the damaged structure conceived in this manner, simulates the realistic behaviour in the conditions of action and of accidental situation and seismic actions, by firstly exposing the structure to the action of the gravitational load, and then by exposing the structure loaded in this way to the accidental action. After that, the vulnerability of the structure is verified on the deformed and damaged structure, while the gravitational load is just transferred from the initial analysis to the following ones and the accidental and seismic action are defined in the corresponding analyses.

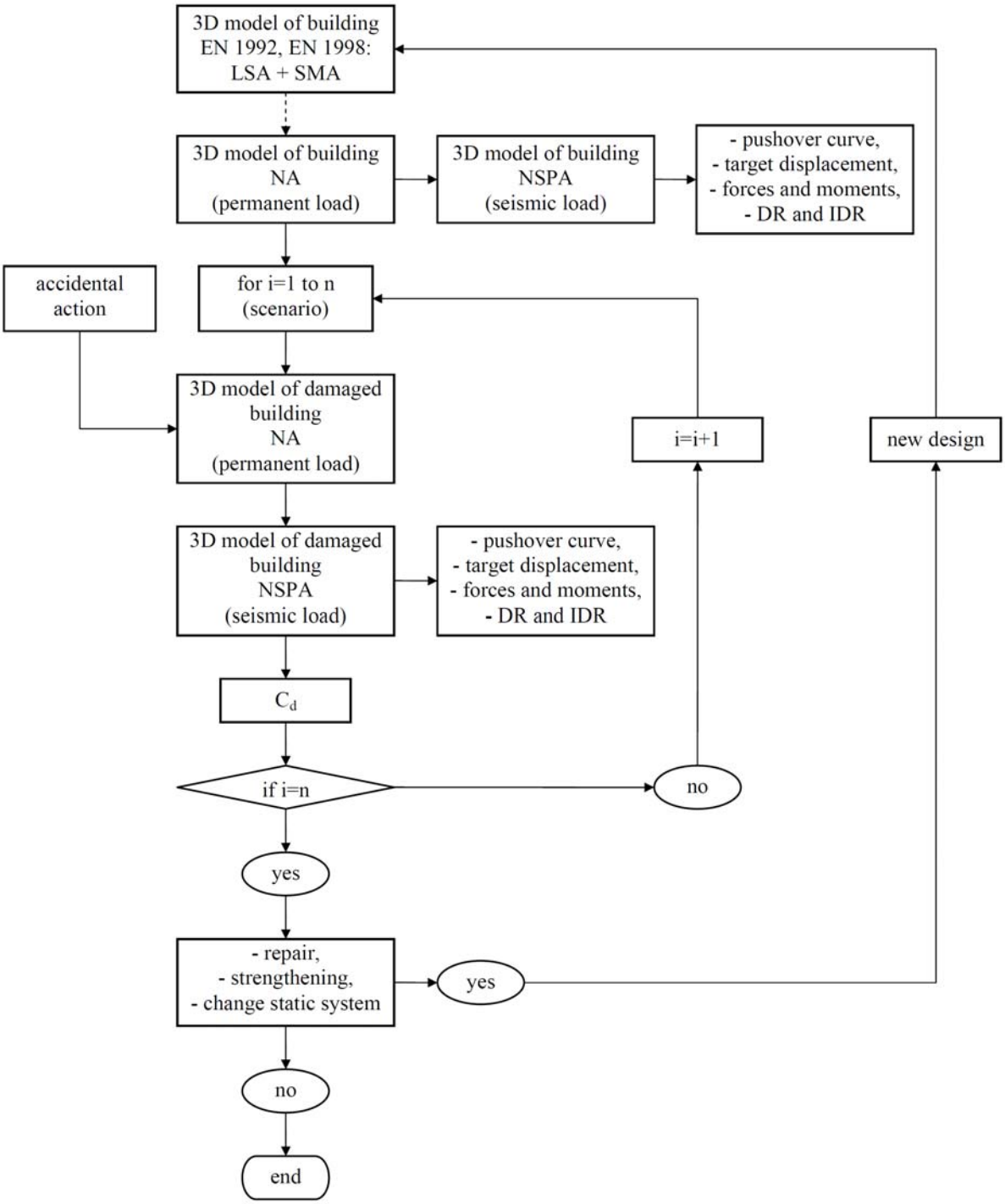

Slika 1. Dijagram toka scenarija povezanih nelinearnih analiza
Figure 1. Flow chart of scenarios of the related non-linear analyses

3 KOEFICIJENT OŠTEĆENJA

Razmatranje stepena oštećenja objekta izloženog incidentnom i seizmičkom dejstvu sprovedeno je uvođenjem novog koeficijenta oštećenja C_d. Ovim koeficijentom sprovodi se uporedna analiza neoštećenog i oštećenog objekta. U odnosu na postojeće indekse oštećenja, koji se zasnivaju na analizi stepena oštećenja objekta izloženog seizmičkom dejstvu i razmatranja odgovora

3 DAMAGE COEFFICIENT

Considerations regarding the degree of damage to the building exposed to accidental and seismic actions were carried out by introducing the damage coefficient C_d. This is the coefficient based on which a comparative analysis between the undamaged and the damaged building is carried out. Unlike the existing damage indices, which are based on analyzing the degree of

sistema u vremenskom domenu, primenom koeficijenta oštećenja C_d razmatra se odgovor sistema u kapacitativnom domenu. U tom smislu se i dobija potpunija slika o stepenu oštećenja objekta, jer se razmatra sistem od inicijalnog elastičnog stanja preko nelinearnog, pa sve do kolapsnog stanja. S druge strane, razmatranjem stepena oštećenja objekta u kapacitativnom domenu, a primenom koeficijenta oštećenja C_d, moguće je obuhvatiti sve nivoe seizmičkog zahteva koji se postavljaju pred konstrukciju. Kada se razmatranje stepena oštećenja sprovodi preko ustaljenih indeksa oštećenja u vremenskom domenu, moguće je istraživanje sprovesti samo za jedan nivo seizmičkog zahteva. Izraz kojim je uveden koeficijent oštećenja C_d zasniva se na uporednoj analizi *pushover* krive neoštećenog i oštećenog objekta. Oštećenja objekta, kao što je već napomenuto, nastaju usled dejstva incidentne situacije i usled seizmičkog dejstva. Za potrebe ovog istraživanja, a dovoljno pouzdano da se može primeniti u slučaju gotovo svih nelinearnih odgovora višespratnih zgrada, definicija koeficijenta oštećenja C_d bazira se na modelu trilinearne *pushover* krive. *Pushover* krive realnih modela zgrada dobijaju se konekcijom većeg broja diskretnih vrednosti iz inkrementalnih nelinearnih situacija. Konekcija se sprovodi primenom linearne ili splajn interpolacije, tako da u ovom drugom slučaju *pushover* kriva ostavlja utisak glatke krive. Primenom modela trilinearne *pushover* krive, može se ili trilinearizovati *pushover* kriva realnog modela zgrade ili se iz *pushover* krive realnog modela zgrade mogu odrediti ključni parametri koji se koriste kao inputi za model trilinearne *pushover* krive. Na slici 2a prikazan je model trilinearne *pushover* krive čije su diskretne vrednosti linearno interpolirane, dok je na slici 2b prikazan isti model trilinearne *pushover* krive čije su diskretne vrednosti splajnom interpolirane. Međusobno odstupanje linearno i splajn interpolirane *pushover* krive realnog modela zgrade znatno je manje, s obzirom na to što se ove krive, kao što je već rečeno, dobijaju konekcijom većeg broja diskretnih vrednosti iz inkrementalnih nelinearnih situacija.

damage to the building subjected to seismic action and considering the system response in the time domain, the damage coefficient C_d approach considers the system response in the capacitive domain. Thus, a more complete picture can be obtained of the damage degree to the building, since it considers the system from its initial state through the non-linear elastic state to the collapse state. However, when considering the damage degree in the capacitive domain using the damage coefficient C_d, it is possible to cover all levels of seismic demand imposed to the structure. When considering the damage degree based on the usual damage indices in the time domain, only a single level of seismic demand can be taken into consideration. The term on which the damage coefficient C_d was introduced is based on the comparative analysis of pushover curves of the undamaged and damaged building. Damage to the building, as already mentioned, are due to the action of an accidental situation and seismic action. For the purposes of this study, the damage coefficient C_d is defined based on the tri-linear pushover curve model, the reliability of which is sufficient to be applied in almost all non-linear responses of multi-storey buildings. Pushover curves of real building models are obtained by connecting a number of discrete values derived from incremental non-linear situations. The connection is carried out by using linear or spline interpolation, so that in the latter case the pushover curve leaves the impression of a smooth curve. Applying the tri-linear pushover curve model enables either to tri-linearize the pushover curve of the real building model or to take the pushover curve of the real building model as a basis for identifying the key parameters used as inputs for the tri-linear pushover curve model. Figure 2a shows the tri-linear pushover curve model whose discrete values are linearly interpolated, while Figure 2b shows the same tri-linear pushover curve model whose discrete values are spline interpolated. The deviation between the linear and spline interpolated pushover curve of the real building model is much lower, since these curves, as already mentioned, are obtained by connecting a number of discrete values of incremental non-linear situations.

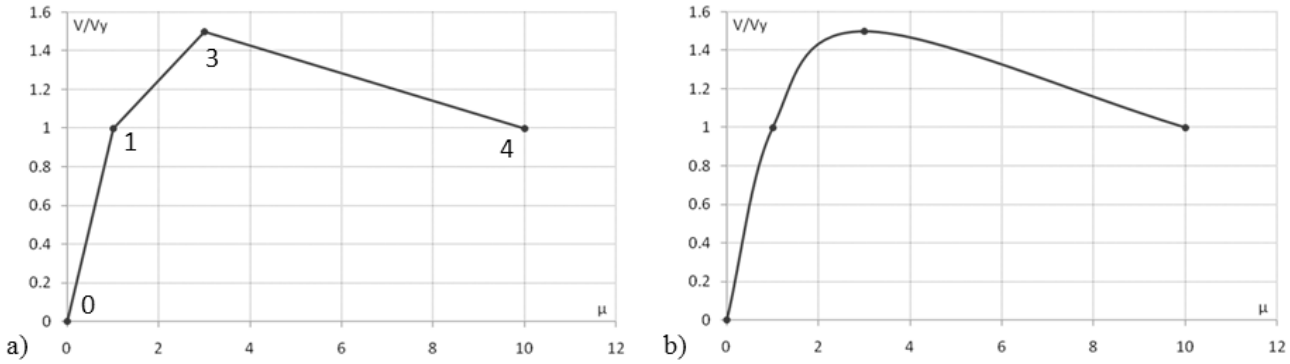

Slika 2. a) model trilinearne pushover krive čije su diskretne vrednosti linearno interpolirane, b) model trilinearne pushover krive čije su diskretne vrednosti splajnom interpolirane
Figure 2. a) tri-linear pushover curve model whose discrete values are linearly interpolated, b) tri-linear pushover curve model whose discrete values are spline interpolated

S ciljem sprovođenja parametarske analize, *pushover* krive su definisane u funkciji koeficijenta duktilnosti μ i odnosa ukupne smičuće sile u osnovi objekta i ukupne smičuće sile u osnovi objekta na granici tečenja V/V_y (relativna ukupna smičuća sila u osnovi objekta). Merodavni parametri modela trilinearne *pushover* krive jesu:

– čvor 1: $0 \le \mu_0 < 1$, $0 \le (V/V_y)_0 < 1$,

– Kao posledica prethodnog incidentnog ili seizmičkog dejstva, inicijalni koeficijent duktilnosti μ_0 i inicijalna relativna ukupna smičuća sila u osnovi objekta $(V/V_y)_0$ mogu biti različiti (veći) od nule, a manji od 1.

– čvor 2: $\mu_y=1$, $(V/V_y)_y=1$,

– Koeficijent duktilnosti na granici tečenja μ_y i relativna ukupna smičuća sila u osnovi objekta na granici tečenja $(V/V_y)_y$ su uvek jednake 1.

– čvor 3: $1<\mu_{h/s}<\mu_{max}$, $(V/V_y)_{h/s}>0$,

– Koeficijent duktilnosti za nivo ojačanja/omekšanja $\mu_{h/s}$ uvek je veći od 1, a manji od koeficijenta maksimalno realizovane duktilnosti μ_{max}, dok je relativna ukupna smičuća sila u osnovi objekta za nivo ojačanja/omekšanja $(V/V_y)_{h/s}$ veća od 0.

– čvor 4: $\mu_{max}>1$, $(V/V_y)_{adeq} \ge 0$,

– Koeficijent maksimalno realizovane duktilnosti μ_{max} uvek je veći od 1, dok je odgovarajuća relativna ukupna smičuća sila u osnovi objekta $(V/V_y)_{adeq}$ veća ili eventualno jednaka 0.

Koeficijent oštećenja C_d definisan je uglavnom u funkciji apsolutnih vrednosti koordinata, ali se, radi sprovođenja parametarske analize, dijagrami *pushover* krivih prikazuju u funkciji relativnih vrednosti koordinata. Uvažavajući prethodno izvedene stavove o ključnim parametrima trilinearne *pushover* krive, ali prevedeni u apsolutne vrednosti koordinata, izveden je koeficijent oštećenja C_d i koji glasi:

In order to conduct the parametric analysis, pushover curves are defined as a function of ductility coefficient μ and the ratio of the total base shear force of the building and the total base shear force of the building at the yield limit V/V_y (the relative total base shear force of the building). Parameters relevant to the tri-linear pushover curve model are the following:

– node 1: $0 \le \mu_0 < 1$, $0 \le (V/V_y)_0 < 1$,

– As a consequence of the previous accidental or seismic action, the initial ductility coefficient μ_0 and the initial relative total base shear force of the building (V/V_y) can be non-zero, i.e. larger than zero and lower than 1.

– node 2: $\mu_y=1$, $(V/V_y)_y=1$,

– The ductility coefficient at the yield limit μ_y and the relative total base shear force of the building at the yield limit (V/V_y) are always equal to 1.

– node 3: $1<\mu_{h/s}<\mu_{max}$, $(V/V_y)_{h/s}>0$,

– The ductility coefficient for the level of hardening/softening $\mu_{h/s}$ is always higher than 1 and lower than the coefficient of maximum realized ductility μ_{max}, while the relative total base shear force of the building for the level of hardening/softening $(V/V_y)_{h/s}$ is higher than 0.

– node 4: $\mu_{max}>1$, $(V/V_y)_{adeq} \ge 0$,

– The coefficient of the maximum realized ductility μ_{max} is always higher than 1, while the adequate relative total base shear force of the building $(V/V_y)_{adeq}$ is higher or equal to 0.

The damage coefficient C_d is generally defined as a function of absolute coordinate values, but for the purpose of parametric analysis, diagrams of pushover curves are presented as a function of relative coordinate values. Taking into account the previously derived positions on key parameters of the tri-linear pushover curve, but translated into absolute coordinate values, the following damage coefficient C_d is derived:

$$C_d = \left| 1 - 0.125 \left[\frac{\int_0^{D_{max,d}} V_d(D_d)\,dD}{\int_0^{D_{max,u}} V_u(D_u)\,dD} + \frac{K_{i,d}}{K_{i,u}} + \frac{K_{n,d}}{K_{n,u}} + \frac{V_{y,d}}{V_{y,u}} + \frac{V_{h/s,d}}{V_{h/s,u}} + \frac{D_{max,d}}{D_{max,u}} + \frac{V_{adeq,d}}{V_{adeq,u}} + \frac{\mu_{max,d}}{\mu_{max,u}} \right] \right|. \quad (3)$$

Koeficijent oštećenja C_d sastoji se iz osam bitnih faktora kojim se definiše stepen oštećenja objekta komparacijom *pushover* krive neoštećenog i oštećenog objekta:

– utvrđivanje stepena oštećenja preko odnosa površi *pushover* krivih neoštećenog $\int V_u(D_u)dD$ i oštećenog objekta $\int V_d(D_d)dD$;

– utvrđivanje stepena oštećenja preko odnosa inicijalne krutosti neoštećenog $K_{i,u}$ i oštećenog objekta $K_{i,d}$;

– utvrđivanje stepena oštećenja preko odnosa nelinearne krutosti neoštećenog $K_{n,u}$ i oštećenog objekta $K_{n,d}$;

– utvrđivanje stepena oštećenja preko odnosa ukupne smičuće sile u osnovi objekta na granici tečenja neoštećenog $V_{y,u}$ i oštećenog objekta $V_{y,d}$;

– utvrđivanje stepena oštećenja preko odnosa ukupne smičuće sile u osnovi objekta za nivo ojačanja/omekšanja neoštećenog $V_{h/s,u}$ i oštećenog

The damage coefficient C_d consists of eight important factors defining the degree of damage to the building by comparing the pushover curves of the undamaged and damaged building:

– determining the degree of damage based on the ratio of the pushover curve surface of the undamaged $\int V_u(D_u)dD$ and the damaged building $\int V_d(D_d)dD$,

– determining the degree of damage based on the ratio of initial stiffness of the undamaged $K_{i,u}$ and the damaged building $K_{i,d}$,

– determining the degree of damage based on the ratio of non-linear stiffness of the undamaged $K_{n,u}$ and the damaged building $K_{n,d}$,

– determining the degree of damage based on the ratio of the total base shear force at the yield limit of the undamaged building $V_{y,u}$ and the damaged building $V_{y,d}$,

– determining the degree of damage based on the ratio of the total base shear force of the building for the level of hardening/softening of the undamaged $V_{h/s,u}$ and

objekta $V_{h/s,d}$;

– utvrđivanje stepena oštećenja preko odnosa maksimalno realizovanog pomeranja neoštećenog $D_{max,u}$ i oštećenog objekta $D_{max,d}$;

– utvrđivanje stepena oštećenja preko odnosa odgovarajuće ukupne smičuće sile u osnovi objekta za maksimalno realizovano pomeranje neoštećenog $(V/V_y)_{adeq,u}$ i oštećenog objekta $(V/V_y)_{adeq,d}$;

– utvrđivanje stepena oštećenja preko odnosa maksimalno realizovanog koeficijenta duktilnosti neoštećenog $\mu_{max,u}$ i oštećenog objekta $\mu_{max,d}$.

Na slici 3 prikazane su *pushover* krive i koeficijenti oštećenja C_d određeni parametarskom analizom, a na osnovu prethodno definisanih parametara. Vrednosti koeficijenti oštećenja su u intervalu C_d=[0,100] i prikazani su u procentima. Ukoliko je koeficijent oštećenja C_d=0%, tada je objekat neoštećen, a ukoliko je koeficijent oštećenja C_d=100%, tada je objekat potpuno oštećen to jest urušen. Povećanjem inicijalnog koeficijenta duktilnosti μ_0 koeficijent oštećenja C_d se malo povećava, u odnosu na model neoštećene zgrade, tako da je čak i pri vrednosti μ_0=1 koeficijent oštećenja C_d=0,6% (slika 3a). S druge strane, povećanjem inicijalne relativne ukupne smičuće sile u osnovi objekta do $(V/V_y)_0$=0,6, koeficijent oštećenja povećava se do C_d=7,5% (slika 3b), tako da se može konstatovati da je koeficijent oštećenja C_d znatno osetljiviji pri promeni inicijalne relativne ukupne smičuće sile u osnovi objekta $(V/V_y)_0$, nego pri promeni inicijalnog koeficijenta duktilnosti μ_0. Povećanjem koeficijenta duktilnosti na granici tečenja na μ_y=2 oštećenog objekta, koeficijent oštećenja se povećava do C_d=13,2% (slika 3c), a redukcijom relativne ukupne smičuće sile u osnovi objekta na granici tečenja do $(V/V_y)_y$=0,4, koeficijent oštećenja se povećava do C_d=16,1% (slika 3d).

damaged building $V_{h/s,d}$,

– determining the degree of damage based on the ratio of maximum realized displacement on undamaged $D_{max,u}$ and damaged building $D_{max,d}$,

– determining the degree of damage based on the ratio of the adequate total base shear force of the building for the maximum realized displacement in the undamaged $(V/V_y)_{adeq,u}$ and the damaged building $(V/V_y)_{adeq,d}$,

– determining the degree of damage based on the ratio of maximum realized ductility coefficient in the undamaged $\mu_{max,u}$ and damaged building, $\mu_{max,d}$.

Figure 3 shows the pushover curves and damage coefficients C_d obtained by parametric analysis and based on the pre-defined parameters. The damage coefficient values are in the interval of C_d=[0,100] and they are shown in percentages. If the damage coefficient is C_d=0%, then the building is undamaged; if the damage coefficient is C_d=100%, then the building suffers total damage - it collapses. By increasing the initial coefficient of ductility μ_0, the damage coefficient C_d slightly increases as compared to the undamaged building model, so that even with μ_0=1, the damage coefficient is C_d=0.6% (Figure 3a). However, increasing the initial relative total base shear force of the building to $(V/V_y)_0$=0.6, the damage coefficient increases to C_d=7.5% (Figure 3b), so it can be concluded that the sensitivity of the damage coefficient C_d is significantly higher when changing the initial relative total base shear force of the building $(V/V_y)_0$ in comparison with changing initial coefficient of ductility μ_0. By increasing the coefficient of ductility at the yield limit to μ_y=2 of the damaged building, the damage coefficient increases to C_d=13.2% (Figure 3c), while by reducing the relative total base shear force of the building at yield limit to $(V/V_y)_y$=0.4, the damage coefficient increases to C_d=16.1% (Figure 3d).

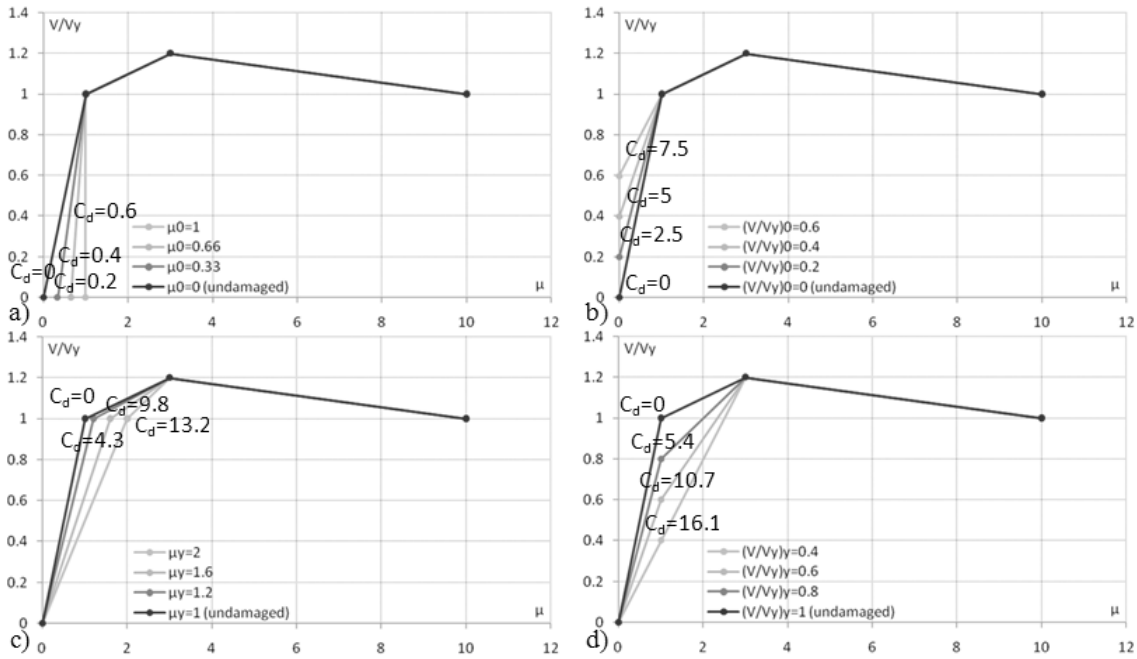

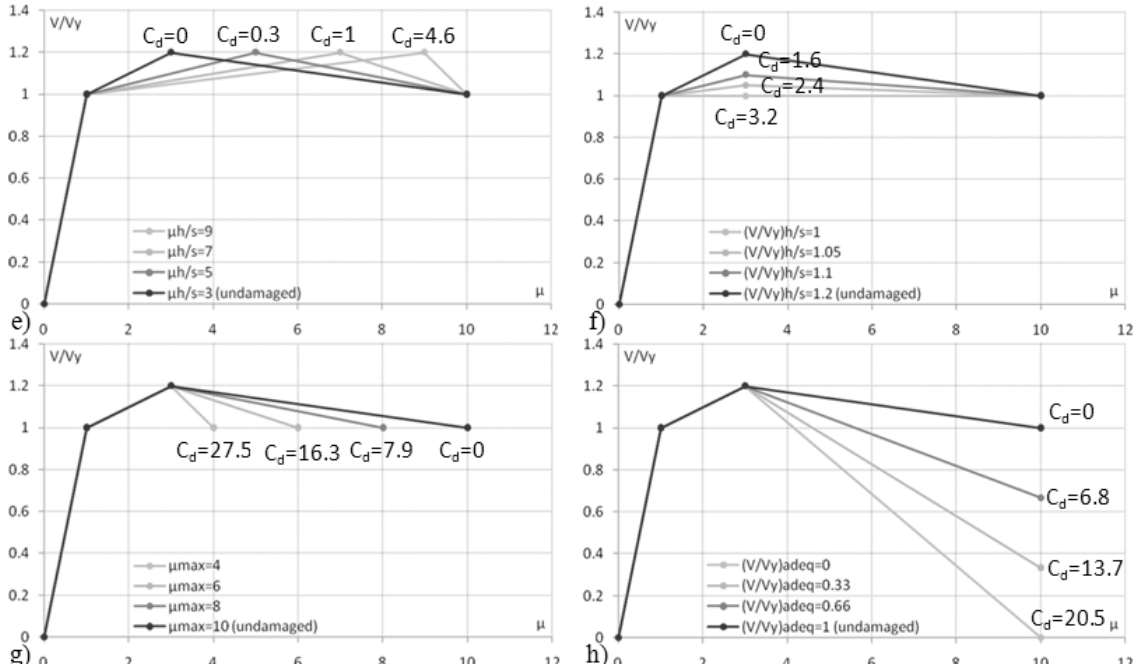

Slika 3. Pushover krive i koeficijenti oštećenja C_d određeni parametarskom analizom: a) inicijalni koeficijent duktilnosti μ_0; b) inicijalna relativna ukupna smičuća sila u osnovi objekta $(V/V_y)_0$; c) koeficijent duktilnosti na granici tečenja μ_y; d) relativna ukupna smičuća sila u osnovi objekta na granici tečenja $(V/V_y)_y$; e) koeficijent duktilnosti za nivo ojačanja/omekšanja $\mu_{h/s}$; f) relativna ukupna smičuća sila u osnovi objekta za nivo ojačanja/omekšanja $(V/V_y)_{h/s}$; g) koeficijent maksimalno realizovane duktilnosti μ_{max}; h) odgovarajuća relativna ukupna smičuća sila u osnovi objekta $(V/V_y)_{adeq}$

Figure 3. Pushover curves and damage coefficients C_d obtained by parametric analysis: a) initial coefficient of ductility μ_0, b) initial relative total base shear force of the building $(V/V_y)_0$, c) coefficient of ductility at yield limit μ_y, d) relative total base shear force of the building at yield limit $(V/V_y)_y$, e) coefficient of ductility for the level of hardening/softening $\mu_{h/s}$, f) relative total base shear force of the building for the level of hardening/softening $(V/V_y)_{h/s}$, g) coefficient of the maximum realized ductility μ_{max}, h) adequate relative total base shear force of the building $(V/V_y)_{adeq}$

Visoke vrednosti koeficijenta duktilnosti za nivo ojačanja/omekšanja $\mu_{h/s}$>6 uslovljavaju i veće oštećenje objekta (slika 3e), dok je pri nižim vrednostima $\mu_{h/s}$ koeficijent oštećenja C_d znatno niži. S druge strane, postepenim povećanjem relativne ukupne smičuće sile u osnovi objekta za nivo ojačanja/omekšanja $(V/V_y)_{h/s}$ i koeficijent oštećenja C_d postepeno se povećava, ali ne disproporcionalno, kao što je to slučaj sa $\mu_{h/s}$ (slika 3f). U odnosu na sve prethodno analizirane parametre, najosetljivijim su se pokazali koeficijent maksimalno realizovane duktilnosti μ_{max} i odgovarajuća relativna ukupna smičuća sila u osnovi objekta $(V/V_y)_{adeq}$. Na slici 3g i 3h prikazane su varijacije ovih parametara i proračunati koeficijenti oštećenja C_d.

High values of the coefficient of ductility for the level of hardening/softening $\mu_{h/s}$>6 also lead to higher damage to the building (Figure 3e), while with lower $\mu_{h/s}$ values, the damage coefficient C_d is much lower. However, a gradual increase in the relative total base shear force of the building for the level of hardening/softening $(V/V_y)_{h/s}$ also leads to the gradual increase in the damage coefficient C_d, but this increase is not disproportional, as it is the case with $\mu_{h/s}$ (Figure 3f). The coefficient of maximum realized ductility μ_{max} and the adequate total relative base shear force of the building $(V/V_y)_{adeq}$ are proven the most sensitive among all analyzed parameters. Figures 3g and 3h show the variation of these parameters and calculated damage coefficients C_d.

4 NUMERIČKE ANALIZE I DISKUSIJA REZULTATA

4.1 Model zgrade

Verifikacija razvijenog scenarija povezanih nelinearnih analiza sprovedena je na primeru desetospratne zgrade okvirnog statičkog sistema. Na slici 4 prikazani su 3D model i osnova desetospratne zgrade. Prethodno je zgrada projektovana prema EN 1992 [8] i EN 1998 [9] propisima, uzimajući u obzir

4 NUMERICAL ANALYSIS AND DISCUSSION

4.1 The building model

Verification of the developed scenario of related non-linear analyses is performed on the example of a 10 storey buildings with a frame static system. The 3D model and layout of a 10 storey building are displayed in figure 4. Previously the building was designed in compliance with EN 1992 [8] and EN 1998 [9] codes,

koncept proračuna prema metodi programiranog ponašanja. Dimenzije zgrade u osnovi su 36x24m, dok su dimenzije jednog polja 6x6m. Visina jednog sprata je 3,3m, a ukupna visina zgrade je 33m. Zgrada je projektovana za beton klase čvrstoće C25/30. Od prizemlja do petog sprata, dimenzije spoljašnjih stubova su 50x60cm, a unutrašnjih 60x70cm, dok su od petog do desetog sprata dimenzije spoljašnjih stubova 40x50cm, a unutrašnjih 50x60cm. Od prizemlja do petog sprata, dimenzije greda su 35x60cm, a od petog do desetog sprata 30x60cm. Debljina ploče svih spratova iznosi 20cm.

taking into consideration the calculation concept according to the *Capacity Design Method*. The floor plan dimensions of the building are 36x24m, while the dimensions of a bay are 6x6m. The total height of the building is 33m, but the height of one storey is 3.3m. The building is designed for concrete class C25/30. From the ground-floor to the fifth storey, the dimensions of the external columns are 50x60cm, and of the internal ones 60x70cm, while from the fifth storey to the tenth storey, dimensions of the external columns are 40x50cm, and of the interior ones 50x60cm. From the ground-floor to the fifth storey, the dimensions of the beams are 35x60cm, and from the fifth storey to the tenth storey they are 30x60cm. The thickness of slabs of all storeys is 20cm.

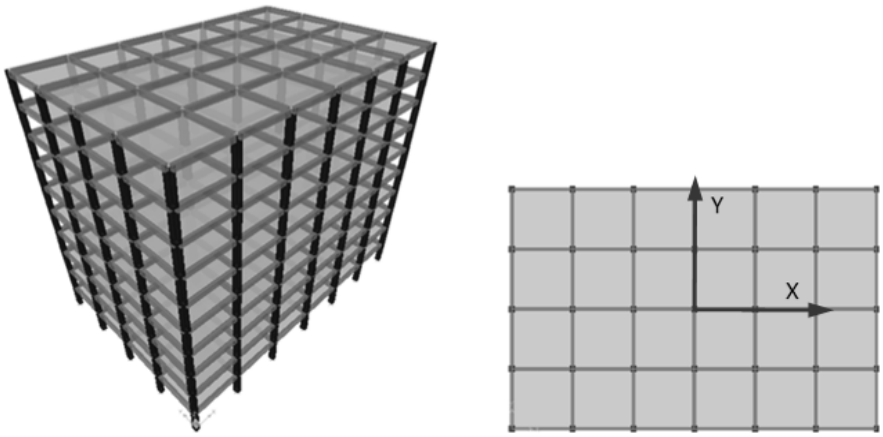

Slika 4. 3D model i osnova desetospratne zgrade
Figure 4. 3D model and layout of the 10-storey building

Opterećenje zgrade računato je kao stalno (sopstvena težina konstruktivnih elemenata zgrade i dodatno stalno opterećenje g=3kN/m²), korisno (povremeno p=3kN/m²) i seizmičko opterećenje. Zgrada je projektovana za povratni period referentnog seizmičkog dejstva od T=475g, projektno ubrzanje tla a_g=0,3g, tip tla C, klasu duktilnosti DCH i faktor ponašanja q=5,85. Zgrada je torziono neosetljiva, s obzirom na to što se centri krutosti poklapaju s centrima masa svih spratova i što se nalaze na jednoj vertikali. Međutim, pri proračunu seizmičkih uticaja dodatno je uzeta vrednost ekscentriciteta od 5% za oba ortogonalna pravca, tako da se za seizmičke kombinacije može smatrati da je zgrada torziono umereno osetljiva. Seizmičke kombinacije su proračunate za bidirekciono dejstvo zemljotresa. Broj svojstvenih oblika koji je uzet u obzir jeste 30, dok su pri proračunu statičkih uticaja uzeti u obzir i *P-Δ* efekti. U svim čvorovima ispunjen je kriterijum da je odnos sume momenata krajeva stubova i sume momenata krajeva greda veći od 1,3. Budući da se konstruktivni sistem zgrade formira od stubova i greda kao linijskih elemenata i ploča kao površinskih elemenata, ovakve zgrade pripadaju grupi neukrućenih i pomerljivih sistema. Za ove sisteme veoma je bitno da se ograniči relativno spratno pomeranje prema $d_r v \leq 0{,}01h$, gde je h visina sprata, v faktor redukcije kojim se uzima u obzir niži povratni period seizmičkog događaja i odnosi se na granično stanje upotrebljivosti, d_r proračunsko međuspratno relativno horizontalno pomeranje, izračunato kao razlika između osrednjenih horizontalnih pomeranja d_s na vrhu i na dnu

The building load is calculated as a permanent one (dead weight of the structural building elements and the additional permanent load g=3kN/m²), useful (live load p=3kN/m²) and seismic load. The building was designed for the return period of reference seismic action of T=475g, design ground acceleration a_g=0.3g, ground type C, ductility class DCH and behaviour factor q=5.85. The building is insensitive to torsion since the stiffness centres coincide with the centres of mass of all the storeys and they are located along one vertical. However, in calculation of seismic effects, and additional value of eccentricity of 5% is assumed for both orthogonal directions, so for the seismic combinations, it can be considered that the building is moderately sensitive in terms of torsion. Seismic combinations are calculated for the bidirectional action of the earthquake. The number of characteristic modes, which was taken in consideration, is 30, while in calculation of the static influences the *P-Δ* effects are taken in consideration as well. In all the nodes, the criterion that the ratio of the sum of the moments on the ends of the columns and the sum of the moments on the ends of the beams is higher than 1.3, is satisfied. Since structural system of the building is formed by columns and beams as linear elements, and slabs as surface elements, such buildings belong to the group of non-stiff and deformable systems. For these systems, it is very important to limit the relative inter-storey drift according to $d_r v \leq 0.01h$, where h is the height of the storey, v is reduction factor which takes into consideration the lower return period of the seismic event and refers to the limit state of serviceability, d_r

posmatranog sprata [9]. Na slici 5a prikazani su globalni driftovi *DR* 3D modela okvirne zgrade proračunati primenom LSA i SMA analiza, čije su maksimalne vrednosti manje od 0,2%, dok su na slici 5b prikazani međuspratni driftovi *IDR* 3D modela okvirne zgrade i granične vrednosti pomeranja prema prethodnom izrazu u funkciji međuspratnog drifta IDR_{EC8} za X i Y pravce. Maksimalne vrednosti međuspratnih driftova manje su od granične vrednosti međuspratnog drifta IDR_{EC8} za v=0,5.

design inter-storey relative horizontal drift, calculated as the difference between mean horizontal drifts d_s at the top and the bottom of the observed storey [9]. The global drifts *DR* of the 3D model of the frame building are presented in Figure 5a; they are calculated using LSA and SMA analyses whose maximum values are lower than 0.2%, while inter-storey drifts *IDR* of the 3D model of frame buildings and ultimate drift values according to the previous expression, in the functions of the inter-storey drift IDR_{EC8} for X and Y directions are presented in the Figure 5b. Maximum values of inter-storey drifts are lower than the limit value of the inter-storey drift IDR_{EC8} for v=0.5.

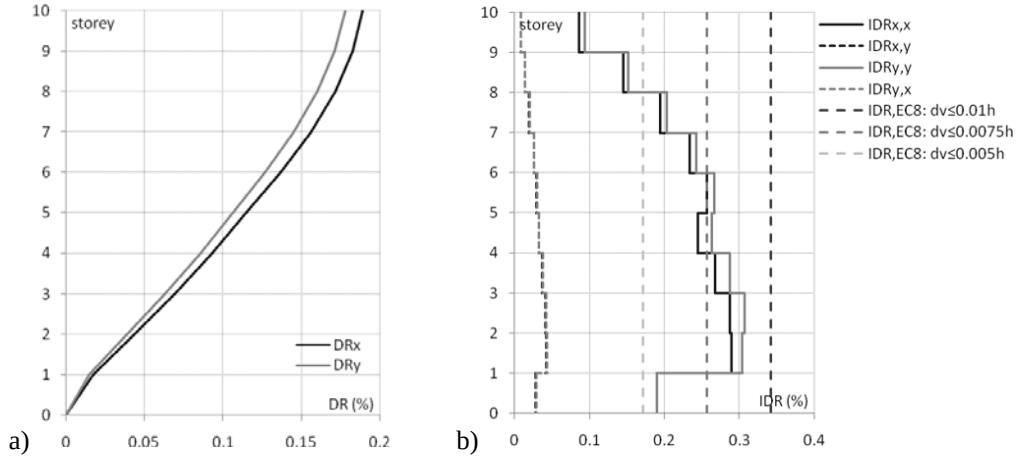

Slika 5. a) globalni driftovi DR; b) međuspratni driftovi IDR 3D modela okvirne zgrade, određeni SMA analizom
Figure 5. a) global drifts DR, b) inter-storey drifts IDR of the 3D frame building model calculated using SMA analysis

4.2 Selekcija i skaliranje akcelerograma

Za potrebe istraživanja prikazanog u ovom radu, korišćeni su akcelerogrami prirodnih zemljotresa koji su se dogodili u prošlosti na teritoriji Srbije i Crne Gore. Akcelerogrami su preuzeti iz evropske baze jakih zemljotresa (ESD) [18] i tretirani su kao neskalirani, a naknadno su skalirani prema zahtevima koji su postavljeni u ovom istraživanju. Svi akcelerogrami su filtrirani eliptičnim pojasnopropusnim filterom, propuštajući frekvencije u intervalu f=[0.25;25]Hz. Zatim je sprovedena korekcija bazne linije primenjujući linearnu funkciju. U tabeli 1 prikazano je deset selektovanih i preuzetih akcelerograma iz ESD baze zemljotresa, gde je M_w momentna magnituda, a *PHA* maksimalno horizontalno ubrzanje.

4.2 Selecting and scaling the accelerograms

For the purpose of the research presented in this paper accelerograms of natural earthquakes that occurred in the past on the territory of Serbia and Montenegro were used. The accelerograms were taken from the *European Strong-Motion Database* (ESD) [18] and they were treated as non-scaled; they were subsequently scaled according to the requirements set out in this research. All accelerograms were filtered using 8th order elliptical bandpass-filter, passing frequencies in the interval of f=[0.25;25]Hz. This was followed by base line correction using linear function. Table 1 shows the ten accelerograms selected and downloaded from the ESD earthquake base, where M_w is the moment magnitude and *PHA* is maximum horizontal acceleration.

Tabela 1. Selektovani i preuzeti akcelerogrami iz ESD baze zemljotresa
Table 1. The selected and downloaded accelerograms from the ESD earthquake base

no.	year	earthquake	station	M_w	*PHA* (m/s²)
1	1979	Montenegro	Petrovac - Hotel Oliva	5.4	0.484
2	1979	Montenegro	Debar - Skupština opštine	6.9	0.599
3	1979	Montenegro	Bar - Skupština opštine	5.8	0.813
4	1979	Montenegro	Petrovac - Hotel Rivijera	6.2	2.703
5	1979	Montenegro	Veliki Ston - Fabrika soli	6.9	2.624
6	1980	Kopaonik	Niš - Škola D. Jovanović	5.9	0.367
7	1980	Kopaonik	Priština - Zavod za urbanizam	5.9	0.293
8	1979	Montenegro (aftershock)	Kotor - Naselje Rakite	6.2	0.56
9	1979	Montenegro	Banja Luka - Borik 9	6.9	0.089
10	1979	Montenegro	Berane - Opština	6.9	0.159

Skaliranje akcelerograma sprovedeno je primenom metode najmanjih kvadrata (LSM), minimizirajući razliku između skaliranog spektra odgovora i projektnog spektra odgovora prema [10]:

The accelerograms were scaled using the *Least Squares Method* (LSM) by minimizing the difference between the scaled response spectrum and the design response spectrum according to [10]:

$$|\Delta| = \int_{T_A}^{T_B} \left[F_s S_{a,us}(T) - S_{a,d}(T) \right]^2 dT \,, \tag{4}$$

gde je F_s faktor skaliranja, $S_{a,us}(T)$ spektralna akceleracija neskaliranog akcelerograma (akcelerogram prirodnog zemljotresa), $S_{a,d}(T)$ spektralna akceleracija projektnog (elastičnog) spektra odgovora prema propisima, T_A i T_B donja i gornja granična vrednost intervala perioda vibracija za koji se sprovodi skaliranje. Određivanje faktora skaliranja sprovodi se minimiziranjem razlike definisane u prethodnom izrazu:

where F_s is the scaling factor, $S_{a,us}(T)$ is the spectral acceleration of the unscaled accelerogram (accelerogram of natural earthquake), $S_{a,d}(T)$ is the spectral acceleration of the design (elastic) response spectrum according to the regulations, T_A and T_B are the lower and upper limits of vibration period interval for which the scaling was conducted. The scaling factor is determined by minimizing the difference defined in the previous expression:

$$\min|\Delta| \Rightarrow \frac{d|\Delta|}{dF_s} = 0 \Rightarrow F_s = \frac{\sum_{T_A}^{T_B} \left(S_{a,us}(T) S_{a,d}(T) \right)}{\sum_{T_A}^{T_B} \left(S_{a,us}(T) \right)^2} \,. \tag{5}$$

U ovom istraživanju korišćen je elastični spektar odgovora prema EN 1998 [9] propisu, u odnosu na koji se sprovodi skaliranje, za maksimalno ubrzanje tla *PGA*=0,3g. Preporuka EN 1998 [9] propisa je da se pri skaliranju razmatra interval perioda vibracija od $0{,}2T_1$ do $2T_1$, pri čemu je T_1 period vibracija za prvi svojstveni oblik. Dodatna kontrola ovog intervala perioda vibracija sprovedena je razmatrajući pri kojem poslednjem periodu vibracija zgrade se dobija da je zbir efektivnih modalnih masa za sve razmatrane svojstvene oblike vibracija veći od 90% od ukupne mase konstrukcije [6]. Donja granica kriterijuma $0{,}2T_1$ koji definiše EN 1998 može se pokazati, u određenim situacijama, kao problematična, ali se u ovom slučaju, naknadnom kontrolom, pokazala kao korektna. Nakon određivanja faktora skaliranja, za svaki akcelerogram pojedinačno (različiti faktori skaliranja), sprovedene su analize spektara odgovora, a zatim je određena srednja vrednost spektra odgovora $S_{a,ave}(T)$. Prema EN 1998 [9] nijedna vrednost osrednjenog elastičnog spektra odgovora izračunatog iz svih akcelerograma, a za interval od $0{,}2T_1$ do $2T_1$, ne sme da bude manja od 90% od odgovarajuće vrednosti elastičnog spektra odgovora. S obzirom na to što je određen broj vrednosti spektralnih akceleracija osrednjenog spektra odgovora $S_{a,ave}(T)$, proračunatog primenom LSM metode, manji od 90% od spektra odgovora prema EN 1998, naknadno je sprovedeno skaliranje osrednjenog spektra odgovora $S_{a,ave}(T)$. Na slici 6a prikazani su spektri odgovora originalnih neskaliranih akcelerograma selektovani i preuzeti iz ESD baze zemljotresa, dok je na slici 6b prikazan projektni elastični spektar odgovora prema EN 1998, 90% projektni elastični spektar odgovora prema EN 1998, osrednjen spektar odgovora skaliranih akcelerograma i naknadno skaliran osrednjen spektar odgovora skaliranih akcelerograma.

The elastic response spectrum according to EN 1998 code [9] was used in this research based on which the scaling was carried out for maximum ground acceleration of *PGA*=0.3g. As recommended in [9], the scaling should be conducted by considering the vibration period interval from $0.2T_1$ to $2T_1$, where T_1 is the vibration period for the first eigenform. The vibration period interval was additionally controlled by identifying the building's last period of vibration for which the sum of effective modal masses for all considered eigenforms of vibration is higher than 90% of the total mass of the structure [6]. In certain circumstances, the lower $0.2T_1$ limit defined by the EN 1998 code can be problematic, but in this case, the additional control has proved it correct. After determining the scaling factor for each accelerogram individually (different scaling factors) the response spectra analyses were carried out, which was followed by the identification of the average response spectrum value $S_{a,ave}(T)$. According to the EN 1998 code [9], no value of an average elastic response spectrum calculated from all accelerograms for the $0.2T_1$ to $2T_1$ interval, should not be lower than 90% of the corresponding value of elastic response spectrum. Given that a number of values of spectral acceleration of the average response spectrum $S_{a,ave}(T)$, as calculated using the LSM method, is lower than 90% of the response spectrum provided in the EN 1998 code, the average response spectrum $S_{a,ave}(T)$ was subsequently scaled. Figure 6a shows the response spectra of the original unscaled accelerograms, selected and downloaded from the ESD earthquake base. Figure 6b shows the design elastic response spectrum according to the EN 1998 code, 90% of the design elastic response spectrum according to the EN 1998 code, the average response spectrum of the scaled accelerograms and their subsequently scaled averaged response spectrum.

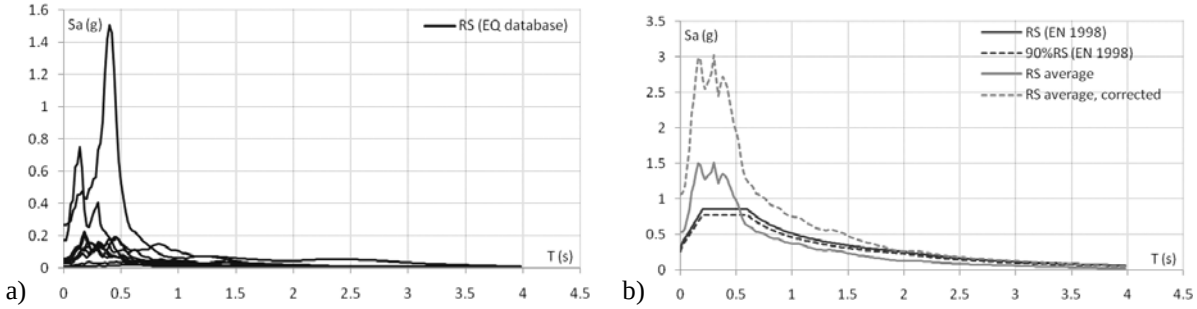

Slika 6. a) spektri odgovora originalnih neskaliranih akcelerograma selektovani i preuzeti iz ESD baze zemljotresa; b) projektni elastični spektar odgovora prema EN 1998, 90% projektni elastični spektar odgovora prema EN 1998, osrednjen spektar odgovora skaliranih akcelerograma i naknadno skaliran osrednjen spektar odgovora skaliranih akcelerograma

Figure 6. a) response spectra of the original unscaled accelerograms selected and downloaded from the ESD earthquake base, b) the design elastic response spectrum according to the EN 1998 code, 90% of the design elastic response spectrum according to the EN 1998 code, the averaged response spectrum of the scaled accelerograms and their subsequently scaled averaged response spectrum

4.3 Scenarija oštećenja zgrade

Scenario kolapsa stubova sproveden je eliminacijom pojedinih stubova u prizemlju desetospratne zgrade. Na slici 7 prikazano je devet scenarija kolapsnih stanja stubova prizemlja, pri čemu su moguće opcije kolapsa u okviru pojedinačnih scenarija:

– scenarija u kojima su prikazana kolapsna stanja samo ivičnih stubova odgovaraju mogućem oštećenju ovih stubova usled terorističkog akta aktiviranjem eksploziva u vozilu postavljenog u neposrednoj blizini zgrade;

– scenarija u kojima su prikazana kolapsna stanja samo unutrašnjih stubova odgovaraju mogućem oštećenju ovih stubova usled terorističkog akta aktiviranjem ekspoziva postavljenog unutar zgrade;

– scenarija u kojima su prikazana kolapsna stanja i unutrašnjih i spoljašnjih stubova odgovaraju mogućem oštećenju ovih stubova usled dejstva snažnih zemljotresa.

4.3 Damage scenarios for the building

The scenario of column collapse was conducted by elimination of individual columns of the ground-floor of a 10-storey building. Nine scenarios of collapse states of ground-floor columns (or sudden removal corner, edge and internal columns) are presented in Figure 7 with the following possible options:

– the scenarios displaying collapse states of outer columns which correspond to the possible damage of columns due to the terrorist action comprising detonation of explosive in a vehicle parked in the immediate vicinity of the building,

– the scenarios displaying collapse states of inner columns which correspond to the potential damage of columns due to the terrorist action comprising detonation of explosive planted inside the building,

– the scenarios displaying collapse states of both interior and exterior columns which correspond to the possible damage of columns due to intensive earthquakes.

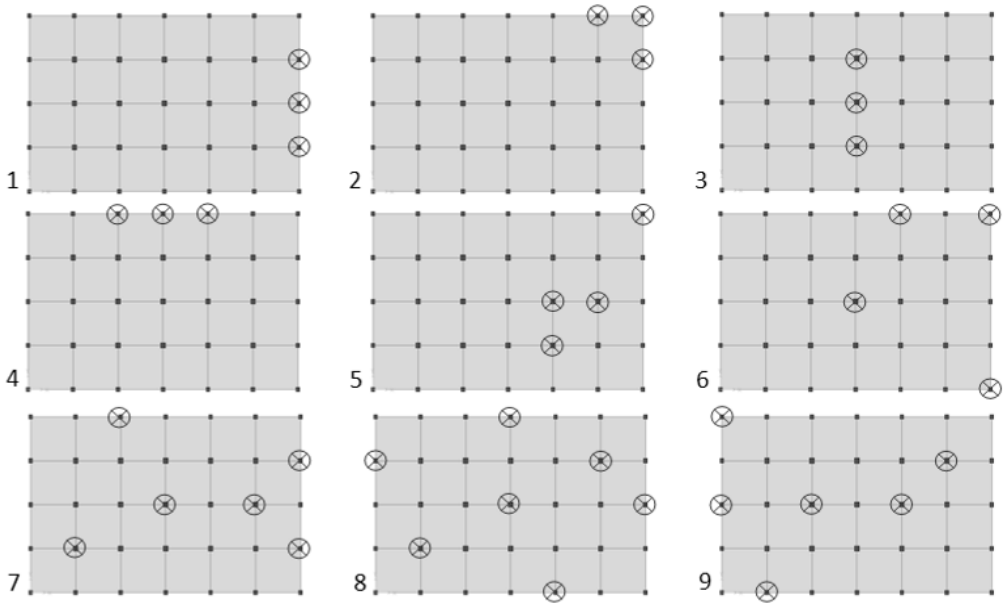

Slika 7. Scenarija oštećenja zgrade (kolaps stubova u prizemlju)
Figure 7. Scenarios of building damage (collapse of ground level columns)

4.4 Postprocesiranja rezultata numeričkih analiza: NSPA *pushover* krive

Razvoj materijalne nelinearnosti se sprovodi preko plastičnih zglobova, pri čemu je kod greda omogućena plastifikacija momentima savijanja, dok je kod stubova omogućena plastifikacija interakcijom momenata savijanja i normalnih sila. Posebno su razmatrana nelinearna ponašanja zgrada za X pravac, a posebno za Y pravac. Za X pravac sproveden je monitoring pomeranja najvišeg čvora zgrade u centru mase za stepen slobode u X pravcu, dok je za Y pravac sproveden monitoring pomeranja najvišeg čvora zgrade u centru mase za stepen slobode u Y pravcu. Prilikom sprovođenja NSPA analiza, za svaki pravac uzeto je u obzir bidirekciono seizmičko dejstvo primenom pravila $1EQ_X+0{,}3EQ_Y$, odnosno $1EQ_Y+0{,}3EQ_X$. Na slici 8 prikazane su NSPA *pushover* krive za sprovedene NSPA analize neoštećene zgrade i devet predefinisanih scenarija.

4.4 Post-processing the results of numerical analyses: NSPA pushover curves

Material non-linearity is developed through plastic hinges, wherein beams are allowed to plastify under the impact of bending moments, while columns are allowed to plastify under the interaction of the bending moment and normal force. The non-linear behaviour of the buildings for the X direction was considered separately from that considered for the Y direction. In the case of the X direction, the displacement of the highest node of the building in the centre of mass for the degree of freedom (DOF) in the X direction was monitored, while in the case of the Y direction the displacement of the highest node of the building in the centre of mass for the degree of freedom in the Y direction was monitored. In the course of performing the NSPA analyses, bidirectional seismic action was assumed for each direction using the rule $1EQ_X+0.3EQ_Y$, i.e. $1EQ_Y+0.3EQ_X$. Figure 8 shows NSPA pushover curves for the pre-defined scenarios and undamaged building.

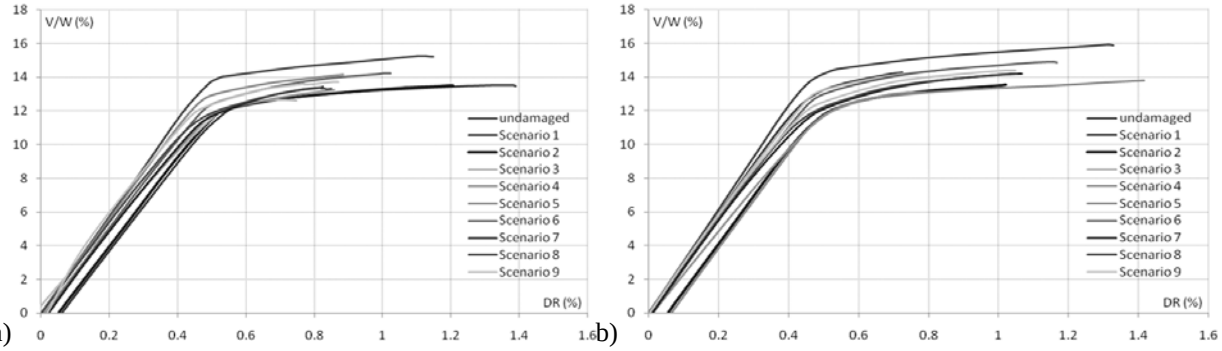

Slika 8. NSPA pushover krive za predefinisana scenarija: a) monitoring pomeranja za stepen slobode u X pravcu, b) monitoring pomeranja za stepen slobode u Y pravcu

Figure 8. NSPA pushover curves for the pre-defined scenarios: a) monitoring displacement for the degree of freedom in the X direction, b) monitoring displacement for the degree of freedom in the Y direction

Razmatrajući nosivost u nelinearnom domenu, kod svih NSPA *pushover* krivih može se konstatovati da je ona najveća kod neoštećene zgrade, što se i moglo očekivati. Međutim, iz aspekta realizovanih nelinearnih pomeranja, maksimalna pomeranja dobijena su u slučaju prvog scenarija za X pravac i četvrtog scenarija za Y pravac. Ovako dobijeni rezultati govore o nivou povredljivosti zgrade u X pravcu kada su oštećeni samo spoljašnji stubovi. Razmatrajući iniciranje krutosti u linearnom domenu, može se konstatovati da ne polaze sve NSPA *pushover* krive od nulte vrednosti. Ovo je posledica primene povezanih nelinearnih analiza kojim se uzima u obzir da su prvo nastupila kolapsna stanja u stubovima, pa je zatim sprovedena NSPA analiza. Prilikom ovakvih scenarija, nivo inicijalnog drifta najčešće je pomeren ka pozitivnoj vrednosti. U određenim slučajevima, nivoi maksimalno realizovanih pomeranja manji su od maksimalno realizovanih pomeranja koja su dobijena kod neoštećene zgrade. U ovim situacijama, kolaps zgrada nastupa ranije, pa što je nivo maksimalno realizovanog pomeranja manji, tim pre i nastupa kolapsno stanje zgrade.

By considering the bearing capacity in the non-linear domain, for all NSPA pushover curves, it can be concluded that it is the highest for the undamaged building, which was to be expected. However, from the aspect of realized non-linear displacements, maximum displacements were obtained in the case of the first scenario for the X direction and the fourth scenario for the Y direction. The results obtained in this way describe the vulnerability level of the building in the case when only outer columns are damaged. Considering initiation of stiffness in the linear domain, it can be stated that not all the NSPA pushover curves start from the zero. This is the result of application of related non-linear analysis, which assumes that NSPA analysis was conducted after the collapse of the columns. For such scenarios, the level of initial drift is most frequently shifted towards the positive value. In certain cases, the levels of maximum realized drifts are lower than the maximum realized drifts obtained for undamaged buildings. In such situations, the collapse of the buildings sets sooner, so the lower the level of maximum realized drift, the sooner the collapse state of the building.

4.5 Postprocesiranja rezultata numeričkih analiza: nivo ciljnog pomeranja

U drugom delu istraživanja sprovedene su analize nivoa ciljnog pomeranja po metodi spektra kapaciteta (CSM) prema ATC 40 [3] propisu za naknadno skaliran osrednjen spektar odgovora skaliranih akcelerograma. U tabeli 2 prikazani su proračunati parametri nivoa ciljnog pomeranja prema CSM metodi za neoštećenu zgradu i moguće scenarije, posebno za X pravac, a posebno za Y pravac. Pored parametara, kao što su nivo ciljnog pomeranja D_t, ukupna smičuća sila u osnovi zgrade za nivo ciljnog pomeranja V_t, efektivan period vibracija za nivo ciljnog pomeranja $T_{eff,t}$ i koeficijent efektivnog prigušenja za nivo ciljnog pomeranja $\xi_{eff,t}$, prikazana su i procentualna odstupanja po scenarijama u odnosu na model neoštećene zgrade. Nivo ciljnog pomeranja nije identičan za neoštećenu zgradu i sva predefinisana scenarija, s obzirom na to što razmatranje i nije sprovedeno za isti nivo ciljnog pomeranja, već za isti nivo seizmičkog zahteva. Efektivan period vibracija za nivo ciljnog pomeranja $\xi_{eff,t}$ odgovara sekantnom periodu vibracija u kapacitativnom domenu, odnosno u formatu spektralno pomeranje-spektralno ubrzanje (ADRS). Ovaj period vibracije znatno je duži od elastičnog perioda vibracija zgrade, budući da se uzima u obzir razvoj elastoplastičnih deformacija u određenim poprečnim presecima. Za X pravac su najproblematičniji treći i sedmi scenario, jer se za nivo seizmičkog zahteva nije moglo realizovati ciljno pomeranje (N/A), odnosno jer je kapacitet nelinearnih deformacija konstrukcije isuviše mali. Za Y pravac su najproblematičniji prvi, treći i peti scenario prilikom kojih se takođe nije moglo realizovati ciljno pomeranje. U slučaju svih scenarija kolapsa stubova vrednosti efektivnog perioda vibracija za nivo ciljnog pomeranja $T_{eff,t}$ se povećavaju, u odnosu na $T_{eff,t}$ kod neoštećene zgrade, dok se ukupna smičuća sila u osnovi zgrade za nivo ciljnog pomeranja V_t po svim scenarijima smanjuje, a nivo ciljnog pomeranja D_t povećava.

4.5 Post-processing the results of numerical analysis: target displacement

In the second part of the research, target displacement analyses were conducted according to the CSM (*Capacity Spectrum Method*) from the ATC 40 [3] codes, assuming the subsequently scaled averaged response spectrum of scaled accelerograms. The calculated target displacement parameters according to the CSM for the undamaged building and possible scenarios, separately for the X direction and separately for the Y direction are presented in Table 2. Departures in percents per scenario, in comparison with the model of the undamaged building are presented apart from the parameters, such as: the level of target displacement D_t, the total base shear force for the target displacement level V_t, effective period of vibrations for the target displacement level $T_{eff,t}$ and coefficient of effective damping for the target displacement level $\xi_{eff,t}$. The level of target displacement is not identical for the undamaged building and all the pre-defined scenarios, as the consideration was not conducted for the same level of target displacement, but the same level of seismic demand. The effective period of vibrations for the target displacement level $\xi_{eff,t}$ corresponds to the second period of vibrations in terms of capacity, i.e. in the ADRS (acceleration-displacement response spectra) format. This period of vibrations is considerably higher than the elastic period of building vibration, since the development of elastic-plastic deformations in certain cross-sections is taken into account. The most problematic scenarios for the X direction are the third and seventh, since for the seismic demand the target displacement could not be realized (N/A), i.e. capacity of non-linear deformations of the structure is too small. The most problematic scenarios for the Y direction are the first, third and fifth scenarios, where target displacement could not be realized, either. For all the scenarios of the column collapse, the values of effective period of vibrations for the target displacement level $T_{eff,t}$ increase, in comparison to $T_{eff,t}$ of the undamaged building. On the other hand, the total base shear force of the building for the target displacement level V_t decreases in all the scenarios, while the level of the target displacement D_t increases.

Tabela 2. Proračunati parametri nivoa ciljnog pomeranja prema CSM metodi za naknadno skaliran osrednjen spektar odgovora skaliranih akcelerograma

Table 2. The calculated parameters of the target displacements according to the CSM method for the subsequently scaled averaged response spectrum of scaled accelerograms

monitoring X DOF								
scenario	D_t (cm)		V_t (kN)		$T_{eff,t}$ (s)		$\xi_{eff,t}$ (%)	
undamaged	26.8		14477.8		2.80		20.8	
1	28.9	+7.8%	12828.3	-11.4%	2.94	+5.0%	20.8	0%
2	28.5	+6.3%	12847.9	-11.3%	2.97	+6.1%	21.0	+1.0%
3	N/A	-	N/A	-	N/A	-	N/A	-
4	27.0	+0.8%	13794.8	-4.7%	2.92	+4.3%	21.3	+2.4%
5	27.9	+4.1%	12976.1	-10.4%	3.02	+7.9%	20.2	-2.9%
6	27.9	+4.1%	13693.6	-5.4%	2.92	+4.3%	21.0	+1.0%
7	N/A	-	N/A	-	N/A	-	N/A	-
8	27.1	+1.1%	13134.7	-9.3%	2.99	+6.8%	21.4	+2.9%
9	26.3	-1.9%	13367.5	-7.7%	2.94	+5.0%	21.7	+4.3%

monitoring Y DOF								
scenario	D_t (cm)		V_t (kN)		$T_{eff,t}$ (s)		$\xi_{eff,t}$ (%)	
undamaged	26.9		14940.1		2.76		20.8	
1	N/A	-	N/A	-	N/A	-	N/A	-
2	29.0	+7.8%	13086.2	-12.4%	2.92	+5.8%	20.4	-1.9%
3	N/A	-	N/A	-	N/A	-	N/A	-
4	29.2	+8.6%	12989.4	-13.1%	2.91	+5.4%	21.0	+1.0%
5	N/A	-	N/A	-	N/A	-	N/A	-
6	28.0	+4.1%	14210.5	-4.9%	2.88	+4.4%	21.1	+1.4%
7	28.1	+4.5%	13622.9	-8.8%	2.97	+7.6%	21.2	+1.9%
8	27.7	+2.9%	13584.8	-9.1%	2.96	+7.3%	20.7	-0.5%
9	27.5	+2.2%	13816.0	-7.5%	2.90	+5.1%	20.7	-0.5%

Nakon određivanja nivoa ciljnog pomeranja po svim scenarijima, proračunati su globalni *DR* i međuspratni driftovi *IDR*, tako što su naknadno procesirane NSPA analize sprovodeći monitoring pomeranja za odgovarajući stepen slobode i odgovarajući pravac do nivoa ciljnog pomeranja svakog scenarija pojedinačno. Zatim su izdvajane vrednosti pomeranja po čvorovima spratova za odgovarajući pravac i određivane maksimalne vrednosti ovih pomeranja po spratovima. Globalni driftovi *DR* za nivo ciljnog pomeranja određeni su prema:

After determining the levels of target displacement for all scenarios, the global *DR* and the inter-storey drifts *IDR* were calculated by post-processing the NSPA analyses based on monitoring displacements for the corresponding degree of freedom and corresponding direction before the level of target displacement for each individual scenario. Then the values of displacement at storey nodes for the corresponding direction were singled out and the maximum values of these displacements at stories identified. Global drifts *DR* for level of target displacement are determined by:

$$DR_{t,i} = \frac{\left|D_{t,i,j,k,max}\right|}{H_i}, \tag{6}$$

gde je $DR_{t,i}$ globalni drift pri nivou ciljnog pomeranja *i*-tog sprata, $D_{t,i,j,k,max}$ maksimalno pomeranje pri nivou ciljnog pomeranja *j*-tog čvora *i*-tog sprata *k*-tog stepena slobode, H_i visina *i*-tog sprata od osnove. Međuspratni driftovi *IDR* za nivo ciljnog pomeranja određeni su prema:

where $DR_{t,i}$ is the global drift at the level of target displacement of the *i*-th storey, $D_{t,i,j,k,max}$ is the maximum displacement at the level of target displacement of *j*-th node of the *i*-th storey of the *k*-th degree of freedom, H_i is the height of the *i*-th storey from the basement. Inter-storey drifts *IDR* for the level of target displacement are determined by:

$$IDR_{t,i} = \frac{\left|D_{t,i+1,j,k,max}\right| - \left|D_{t,i,j,k,max}\right|}{H_{i+1} - H_i}, \tag{7}$$

gde je $IDR_{t,i}$ međuspratni drift pri nivou ciljnog pomeranja *i*-tog sprata. Na slici 9 prikazani su globalni driftovi *DR* za X i Y pravac pri nivou ciljnog pomeranja 3D modela okvirne zgrade, određeni za isti nivo seizmičkog zahteva. Maksimalne vrednosti globalnog drifta za X i Y pravac neoštećene zgrade najniže su u odnosu na sva razmatrana scenarija. Takođe, i ostale vrednosti globalnih driftova neoštećene zgrade su manje, u odnosu na sva razmatrana scenarija, izuzev manjeg odstupanja od drugog do šestog sprata petog scenarija X pravca. U slučaju trećeg i sedmog scenarija X pravca i prvog, trećeg i petog scenarija Y pravca, nisu realizovane vrednosti nivoa ciljnog pomeranja, tako da su i odgovarajuće vrednosti globalnih driftova izjednačene sa nulom.

where $IDR_{t,i}$ is inter-storey drift at the level of target displacement of the *i*-th storey. Figure 9 shows the global drifts *DR* for the X and Y directions at the level of target displacement of the 3D frame building model for the same level of seismic demand. Maximum values of the global drift for the X and Y directions of the undamaged building are the lowest of all scenarios taken into consideration. Other values of global drifts of undamaged building are also lower than in all other scenarios considered, except for a slight deviation between the second to the sixth storey of the fifth scenario of X direction. In the cases of the third and seventh scenario of X direction and the first, third and fifth scenarios of Y direction, values at the level of target displacement were unrealized, so that the corresponding values of global drifts are equal to zero.

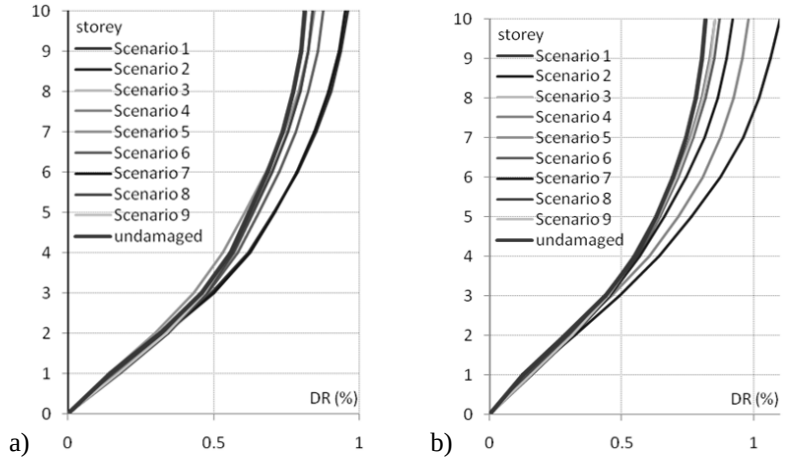

Slika 9. Globalni driftovi DR pri nivou ciljnog pomeranja 3D modela okvirne zgrade, određeni za isti nivo seizmičkog zahteva: a) X pravac; b) Y pravac

Figure 9. Global drifts DR at the level of target displacement of the 3D frame building model, obtained for the same level of seismic demand: a) X direction, b) Y direction

Na slici 10 prikazani su međuspratni driftovi *IDR* za X i Y pravac pri nivou ciljnog pomeranja 3D modela okvirne zgrade, određeni za isti nivo seizmičkog zahteva. Međuspratni driftovi neoštećene zgrade su minimalni od četvrtog do desetog sprata, dok su kod nižih spratova, samo u određenim scenarijima, realizovane još niže vrednosti međuspratnih driftova. Međutim, u svim scenarijima ukupna smičuća sila u osnovi zgrade za nivo ciljnog pomeranja jeste niža, a čime je smanjena nosivost zgrade u nelinearnom domenu, nego što je to slučaj kod neoštećene zgrade. Ovo se može najbolje sagledati pomoću tabele 2, gde su prikazana procentualna odstupanja ukupne smičuće sile u osnovi zgrade. Na primer, u slučaju scenarija 1, gde su eliminisana samo tri ivična stuba u prizemlju zgrade, ukupna smičuća sila u osnovi zgrade je redukovana i više od 11%.

Figure 10 shows the inter-storey drifts *IDR* for X and Y directions at the level of target displacement of the 3D frame building model, obtained for the same level of seismic demand. Inter-storey drifts of the undamaged building are minimal between the fourth to the tenth storey, while in lower stories only in certain scenarios were realized even lower values of inter-storey drift. However, in all scenarios, for the level of target displacement, the total base shear force of the building is lower than in the undamaged building, thus reducing its bearing capacity in the non-linear domain. This can be best seen in table 2, where the percentages of deviations of the total base shear force of the building are shown. For example, in the case of scenario 1, where only three bounding columns on the ground-floor were eliminated, the total base shear force of the building is reduced even by more than 11%.

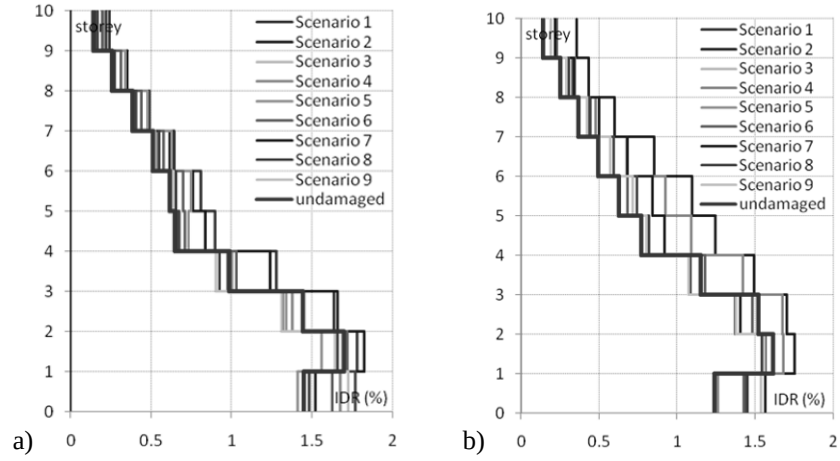

Slika 10. Međuspratni driftovi IDR pri nivou ciljnog pomeranja 3D modela okvirne zgrade, određeni za isti nivo seizmičkog zahteva: a) X pravac; b) Y pravac

Figure 10. Inter-storey drifts IDR at the level of target displacement of the 3D frame building model obtained for the same level of seismic demand: a) X direction, b) Y direction

4.6 Postprocesiranja rezultata numeričkih analiza: maksimalno realizovan nivo pomeranja

U trećem delu istraživanja sprovedene su analize maksimalno realizovanog nivoa pomeranja (kolapsno stanje), pri čemu su u tabeli 3 prikazani proračunati parametri za neoštećenu zgradu i moguće scenarije, posebno za X pravac, a posebno za Y pravac. Pored parametara, kao što su maksimalno realizovan nivo pomeranja D_{max}, ukupna smičuća sila u osnovi zgrade za maksimalno realizovan nivo pomeranja V_{max}, efektivan period vibracija za maksimalno realizovan nivo pomeranja $T_{eff,max}$ i koeficijent efektivnog prigušenja za maksimalno realizovan nivo pomeranja $\xi_{eff,max}$, prikazana su procentualna odstupanja po scenarijama u odnosu na model neoštećene zgrade. U ovom slučaju, procentualna odstupanja $T_{eff,max}$ i $\xi_{eff,max}$ nisu jednoznačna, već su i pozitivna i negativna, s obzirom na to što se dostižu maksimalna pomeranja po scenarijima, koja su i veća i manja od maksimalnih pomeranja neoštećene zgrade. Ukupna smičuća sila u osnovi zgrade za maksimalno realizovan nivo pomeranja V_{max} manja je prilikom svih scenarija, u odnosu na V_{max} neoštećene zgrade. Slična situacija je i kod maksimalno realizovanog nivoa pomeranja D_{max}, osim za prvi i drugi scenario X pravca i četvrti scenario Y pravca.

4.6 Post-processing the results of numerical analyses: the maximum realized level of displacement

Global *DR* and inter-storey drifts *IDR* for the maximum realized level of displacement (collapse state) are considered in the third part of the paper. The calculated parameters of the maximum realized displacement for the undamaged building and possible scenarios, separately for the X direction and separately for the Y direction are presented in table 3. Departures in percents per scenario, in comparison with the model of the undamaged building are presented apart from the parameters such as: maximum realized displacement D_{max}, total base shear force for the maximum realized displacement V_{max}, effective period of vibrations for the maximum realized displacement $T_{eff,max}$ and coefficient of effective damping for the maximum realized displacement $\xi_{eff,max}$,. In this case the percentages of deviations of $T_{eff,max}$ and $\xi_{eff,max}$ are not uniform (unequivocal), but they are both positive and negative since the maximum displacements are reached in the scenarios, which are both higher and lower than the maximum displacements of the undamaged building. The total base shear force for the maximum realized displacement V_{max} is lower in all the scenarios in comparison with the V_{max} of the undamaged building. The situation is similar for the maximum realized level of displacement D_{max}, except for the first and second scenario of the X directions and fourth scenario of the Y direction.

Tabela 3. Proračunati parametri maksimalno realizovanog nivoa pomeranja (kolapsno stanje)
Table 3. Calculated parameters for the maximum realized displacement (collapse state)

monitoring X DOF								
scenario	D_{max} (cm)		V_{max} (kN)		$T_{eff,max}$ (s)		$\xi_{eff,max}$ (%)	
undamaged	37.9		14970.3		3.29		24.6	
1	45.9	+21.1%	13275.6	-11.3%	3.67	+11.6%	25.4	+3.3%
2	39.2	+3.4%	13928.3	-6.9%	3.02	-8.2%	22.4	-8.9%
3	24.7	-34.8%	12417.1	-17.1%	2.84	-13.7%	19.2	-21.9%
4	29.9	-21.1%	13273.8	-11.3%	3.48	+5.8%	24.6	0%
5	28.3	-25.3%	13011.5	-13.1%	3.05	-7.3%	20.6	-16.3%
6	33.8	-10.8%	13990.0	-6.5%	3.20	-2.7%	23.6	-4.1%
7	27.2	-28.2%	13206.4	-11.8%	2.95	-10.3%	21.1	-14.2%
8	28.1	-25.9%	13122.8	-12.3%	3.06	-7.0%	22.3	-9.3%
9	28.7	-24.3%	13491.5	-9.9%	3.07	-6.7%	22.9	-6.9%
monitoring Y DOF								
scenario	D_{max} (cm)		V_{max} (kN)		$T_{eff,max}$ (s)		$\xi_{eff,max}$ (%)	
undamaged	43.8		15634.8		3.41		24.9	
1	23.9	-45.4%	14040.0	-10.2%	2.71	-20.5%	18.3	-26.5%
2	33.7	-23.1%	13303.7	-14.9%	3.14	-7.9%	22.9	-8.0%
3	27.0	-38.3%	14115.8	-9.7%	2.89	-15.2%	20.7	-16.9%
4	46.7	+6.6%	13564.0	-13.2%	3.61	+5.9%	25.1	+0.8%
5	26.1	-40.4%	12875.6	-17.6%	2.88	-15.5%	18.5	-25.7%
6	38.5	-12.1%	14631.9	-6.4%	3.33	-2.4%	24.5	-1.6%
7	35.2	-19.6%	13976.1	-10.6%	3.29	-3.5%	23.9	-4.0%
8	34.7	-20.8%	13949.0	-10.8%	3.28	-3.8%	23.8	-4.4%
9	34.6	-21.0%	14164.9	-9.4%	3.22	-5.6%	23.7	-4.8%

Globalni driftovi *DR* za maksimalno realizovan nivo pomeranja (kolapsno stanje) određeni su prema:

Global drifts *DR* for maximum realized displacements (collapse state) are determined by:

$$DR_{max,i} = \frac{\left|D_{max,i,j,k,max}\right|}{H_i}, \tag{8}$$

gde je $DR_{max,i}$ globalni drift za maksimalno realizovan nivo pomeranja *i*-tog sprata, $D_{max,i,j,k,max}$ maksimalno pomeranje *j*-tog čvora za maksimalno realizovan nivo pomeranja *i*-tog sprata *k*-tog stepena slobode. Međuspratni driftovi *IDR* za maksimalno realizovan nivo pomeranja (kolapsno stanje) određeni su prema:

where $DR_{max,i}$ is the global drift for the maximum realized level of displacement of the *i*-th storey, $D_{max,i,j,k,max}$ is maximum displacement of the *j*-th node for maximum realized level of displacement of the *j*-th storey of the *k*-th degree of freedom. Inter-storey drifts *IDR* for maximum realized displacement (collapse state) are determined by:

$$IDR_{max,i} = \frac{\left|D_{max,i+1,j,k,max}\right| - \left|D_{max,i,j,k,max}\right|}{H_{i+1} - H_i}, \tag{9}$$

gde je $IDR_{max,i}$ međuspratni drift za maksimalno realizovan nivo pomeranja *i*-tog sprata. Na slici 11 prikazani su globalni driftovi *DR* za X i Y pravac pri maksimalno realizovanom nivou pomeranja 3D modela okvirne zgrade. Razmatrajući globalne driftove *DR* može se konstatovati da su veći u slučaju prvog i drugog scenarija X pravca i četvrtog scenarija Y pravca, u odnosu na globalne driftove neoštećene zgrade. Svi ostali globalni driftovi su manji. To jasno ukazuje na to da se kolapsna stanja razvijaju mnogo ranije, nego što je to slučaj kod neoštećene zgrade, osim u slučaju prvog i drugog scenarija X pravca i četvrtog scenarija Y pravca, gde je vrednost duktilnosti povećana, ali je zato znatno smanjena nosivost kompletne zgrade u nelinearnom domenu.

where $IDR_{max,i}$ is inter-storey drift for maximum realized level of displacement of the *i*-th storey. Figure 11 shows global drifts *DR* for X and Y directions at maximum displacement realized for 3D frame building model. When considering global drifts *DR*, it can be concluded that they are higher in cases of the first and second scenarios in the X direction and the fourth scenario in the Y direction, compared to the global drifts of undamaged building. All other global drifts are smaller. This clearly indicates that collapse states develop much earlier than in undamaged building, except in cases of the first and second scenario in the X direction and the fourth scenario in the Y direction, where the value of ductility is increased, but the bearing capacity of the entire building in the non-linear domain significantly reduced.

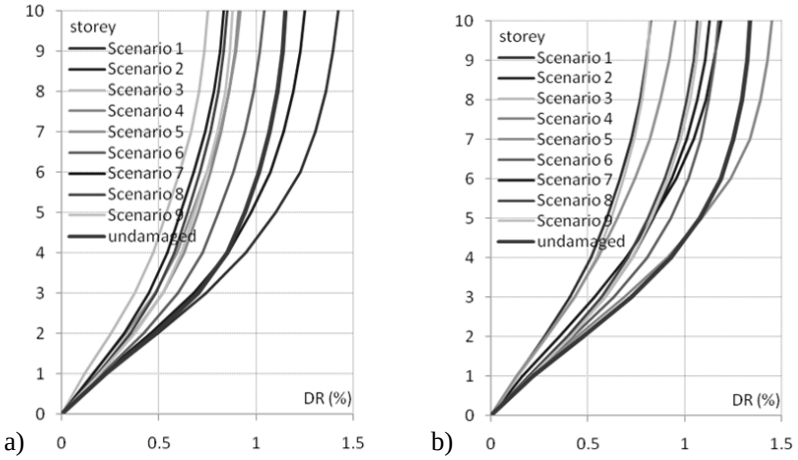

Slika 11. Globalni driftovi DR za maksimalno realizovan nivo pomeranja (kolapsno stanje) 3D modela okvirne zgrade: a) X pravac; b) Y pravac

Figure 11. Global drifts DR for the maximum realized displacement (collapse state) of the 3D frame building model: a) X direction, b) Y direction

Na slici 12 prikazani su međuspratni driftovi *IDR* za X i Y pravac za maksimalno realizovan nivo pomeranja 3D modela okvirne zgrade. Međuspratni driftovi *IDR* takođe ukazuju na veće vrednosti od prizemlja do šestog sprata u slučaju prvog i drugog scenarija X pravca i četvrtog scenarija Y pravca. Međutim, svi međuspratni driftovi iznad šestog sprata su gotovo veći od međuspratnih driftova neoštećene zgrade. To jasno ukazuje na činjenicu da se prilikom svih scenarija pri kolapsnim

Figure 12 shows the inter-storey drifts *IDR* in X and Y directions for the maximum realized displacements for the 3D frame building model. Inter-storey drifts *IDR* also indicate higher values between the ground and the sixth storey in the first and second scenario in the X direction and the fourth scenario in the Y direction. However, all inter-storey drifts above the sixth storey are almost bigger than those in the undamaged building. This clearly points to the fact that in all collapse-state

stanjima razvijaju veće vrednosti međuspratnih driftova kod viših spratova. Od prizemlja do šestog sprata, međuspratni driftovi su manji u slučaju svih scenarija, osim prilikom prvog i drugog scenarija X pravca i četvrtog scenarija Y pravca, mada se i oni smanjuju kod prizemlja i prvog sprata. Niže vrednosti međuspratnih driftova ukazuju na manji nivo povredljivosti zidova ispune zgrade. Međutim, ove vrednosti međuspratnih driftova treba razmatrati u korelaciji s realizovanim globalnim driftovima zgrade. Kao što je već utvrđeno, svi globalni driftovi niži su od globalnih driftova neoštećene zgrade, osim prilikom prvog i drugog scenarija X pravca i četvrtog scenarija Y pravca, tako da veće vrednosti ovih međuspratnih driftova nije ni moguće realizovati, jer nastupa rano kolapsno stanje.

scenarios, higher inter-storey drifts occur at higher stories. Between the ground and the sixth storey, inter-storey drifts are lower in all scenarios, except for the first and second scenario in the X direction and the fourth scenario in the Y direction, although they also decrease at the ground and first storey. Lower values of inter-storey drifts indicate lower levels of vulnerability of the building's infill walls. However, these values of inter-storey drifts should be considered in correlation with the building's realized global drifts. As already noted, all global drifts are lower than those in the undamaged building, except for the first and second scenario in the X direction and the fourth scenario in the Y direction, so that higher values for these inter-storey drifts cannot be realized since the early appearance of collapse state.

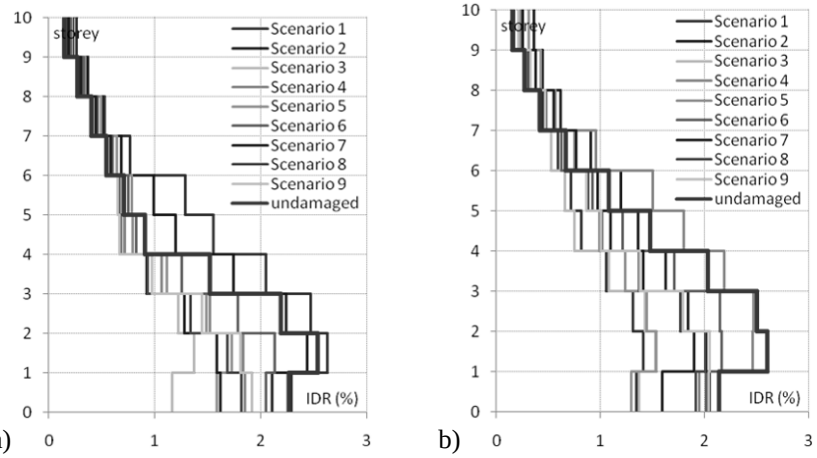

Slika 12. Međuspratni driftovi IDR za maksimalno realizovan nivo pomeranja (kolapsno stanje) 3D modela okvirne zgrade: a) X pravac, b) Y pravac
Figure 12. Inter-storey drifts IDR for the maximum realized displacements (collapse state) of the 3D frame building model: a) X direction, b) Y direction

4.7 Postprocesiranja rezultata numeričkih analiza: analiza oštećenja

U četvrtom delu istraživanja proračunati su koeficijenti oštećenja C_d za sve predefinisane scenarije. Na slici 13 prikazani su trilinearni splajnom interpolirani modeli originalnih *pushover* krivih za X pravac za devet predefinisanih scenarija oštećenja zgrade. Takođe, prikazani su i koeficijenti oštećenja C_d u procentima. U slučaju prvog scenarija, koeficijent oštećenja C_d jeste najniži, pri čemu postoji značajno odstupanje oštećene u odnosu na neoštećenu zgradu. Smanjena je vrednost nosivosti u nelinearnom domenu i postoji inicijalno pomeranje usled kolapsa stubova prizemlja. Međutim, vrednost maksimalno realizovane duktilnosti oštećene zgrade, prema ovom scenariju, jeste veća od vrednosti maksimalno realizovane duktilnosti neoštećene zgrade. Ova činjenica ukazuje na to da je usled povećanja duktilnosti sistema disipacija histerezisne energije veća, pa s obzirom na tu činjenicu, procena ukupnog oštećenja zgrade je na nižem nivou. U odnosu na prvi i drugi scenario, gde su realizovne veće maksimalne duktilnosti sistema, prilikom ostalih scenarija realizovane su manje vrednosti duktilnosti sistema. Tako, na primer,

4.7 Post-processing the results of numerical analyses: damage analysis

In the fourth part of the research damage coefficients C_d for all pre-defined scenarios were calculated. Figure 13 shows the tri-linear spline interpolated models of the original pushover curves in X direction for the nine pre-defined damage scenarios. Damage coefficients C_d are also presented in percentages. Damage coefficient C_d is the lowest in the case of the first scenario, whereby there is a significant deviation between the damaged and the undamaged building. The value of load bearing capacity in the non-linear domain is reduced and there is an initial displacement due to the collapse of ground-floor columns. However, in this scenario, the value of maximum realized ductility of the damaged building is higher than the value of maximum realized ductility of the undamaged building. This fact indicates that higher system ductility leads to higher dissipation of hysteresis energy, so that assessed damage to the building is lower. Compared to the first and the second scenario, where higher maximum system ductility values were realized, in other scenarios lower system ductility values were realized. Thus, for example, the highest value of

u slučaju trećeg scenarija, dobijena je najviša vrednost koeficijenta oštećenja C_d, s obzirom na to što je realizovana najniža vrednost maksimalne duktilnosti i najniža vrednost nosivosti u nelinearnom domenu.

damage coefficient C_d is obtained for the third scenario, given the lowest maximum realized ductility value, and the lowest bearing capacity value in the non-linear domain.

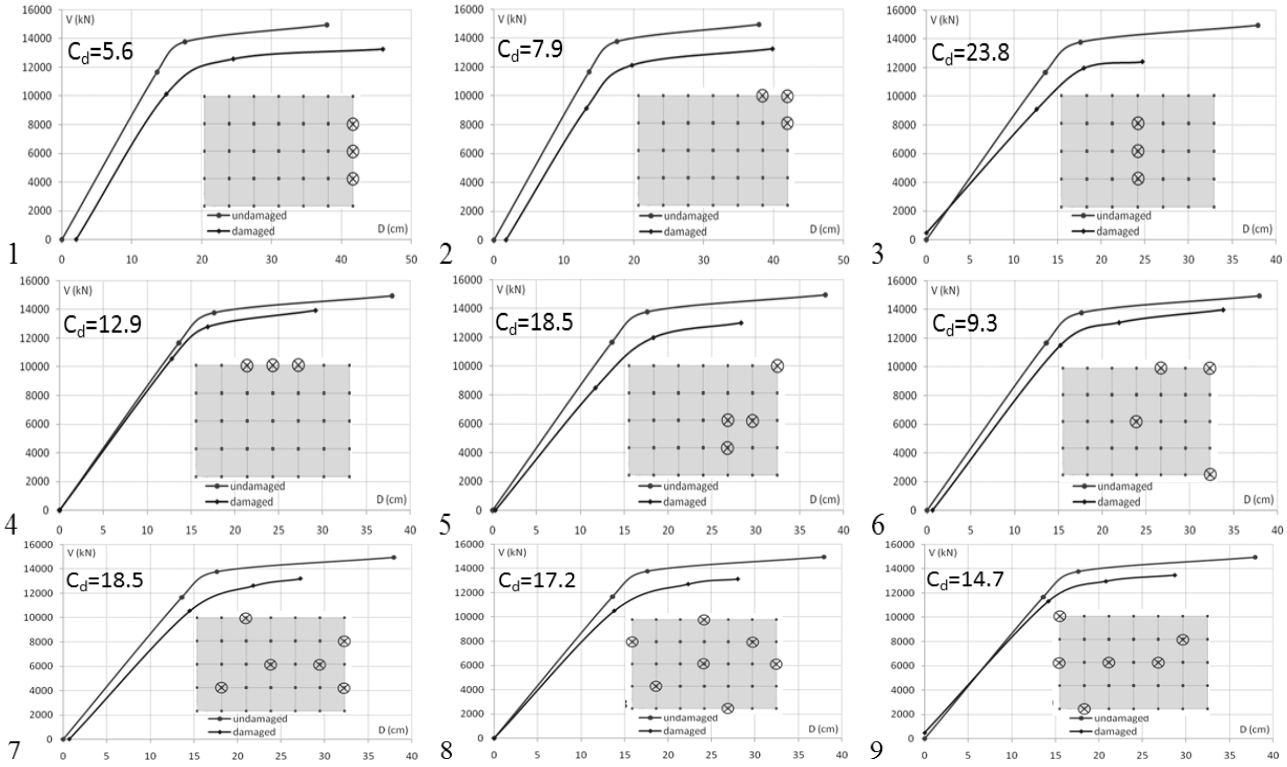

Slika 13. Trilinearni splajnom interpolirani modeli originalnih pushover krivih za X pravac za predefinisana scenarija oštećenja zgrade (kolaps stubova u prizemlju)

Figure 13. Tri-linear spline interpolated models of original pushover curves in X direction for pre-defined damage scenarios (collapse of the ground-floor columns)

Na slici 14 prikazani su trilinearni splajnom interpolirani modeli originalnih *pushover* krivih za Y pravac za devet predefinisanih scenarija oštećenja zgrade. U slučaju četvrtog scenarija, koeficijent oštećenja C_d jeste najniži, pri čemu postoji značajno odstupanje oštećene u odnosu na neoštećenu zgradu. Slično kao kod prvog scenarija, za X pravac i ovde je smanjena vrednost nosivosti u nelinearnom domenu uz postojanje inicijalnog pomeranja usled kolapsa stubova prizemlja. U odnosu na četvrti scenario, gde su realizovne veće maksimalne duktilnosti sistema, prilikom ostalih scenarija realizovane su manje vrednosti duktilnosti sistema. Prilikom petog scenarija dobijena je naveća vrednost koeficijenta oštećenja C_d, budući da je ovde realizovana najniža vrednost maksimalne duktilnosti, uz smanjenu nosivost sistema u nelinearnom domenu.

Figure 14 presents the tri-linear spline interpolated models of original pushover curves in Y direction for nine pre-defined damage scenarios. Damage coefficients C_d are the lowest in the case of the fourth scenario, whereby there is a significant deviation between the damaged and undamaged building. Similar to the case in the first scenario in X direction, the value of the load bearing capacity in the non-linear domain is also reduced and there is also an initial displacement induced by the collapse of ground-floor columns. Compared to the fourth scenario, where higher maximum system ductility values were realized, in other scenarios lower system ductility values were realized. The highest value of damage coefficient C_d is obtained for the fifth scenario, given the lowest maximum realized ductility value, accompanied by reduced bearing capacity of the system in the non-linear domain.

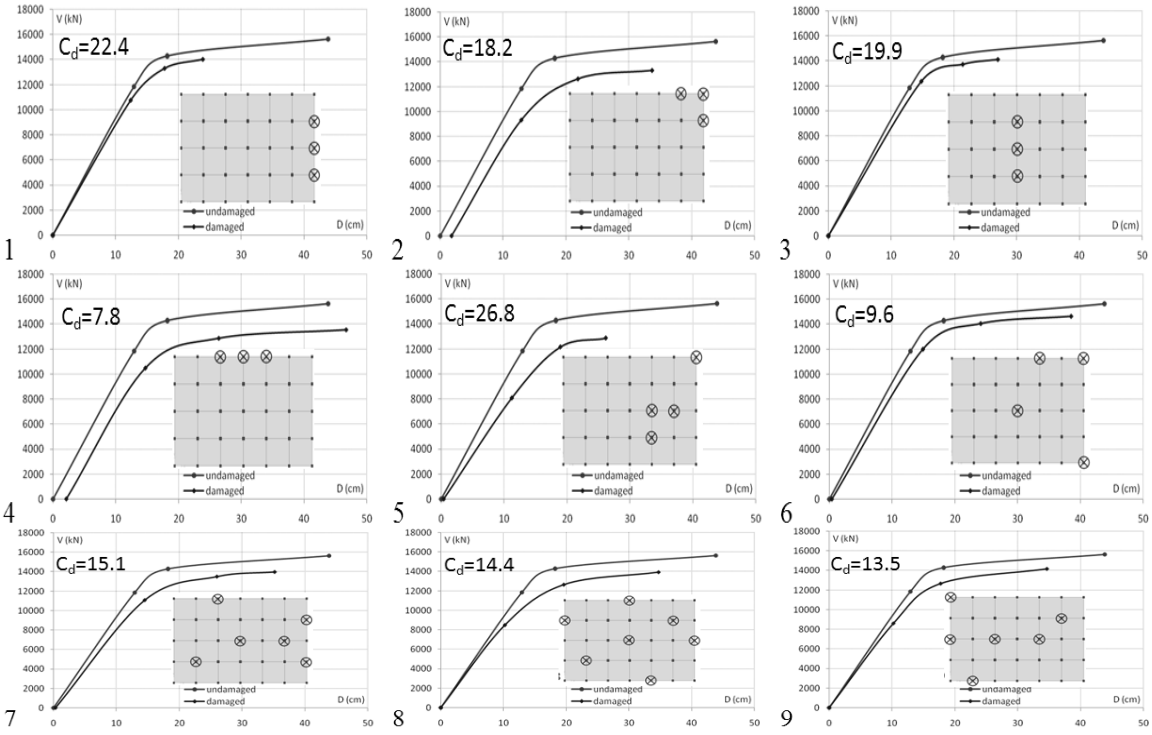

Slika 14. Trilinearni splajnom interpolirani modeli originalnih pushover krivih za Y pravac za predefinisana scenarija oštećenja zgrade (kolaps stubova u prizemlju)

Figure 14. Tri-linear spline interpolated models of original pushover curves in Y direction for pre-defined damage scenario (collapse of the ground-floor columns)

5 ZAKLJUČAK

Na osnovu razvijene metodologije i sprovedenih nelinearnih numeričkih analiza 3D modela zgrade, utvrđeno je da su globalni driftovi pri nivou ciljnog pomeranja, a određeni za isti nivo seizmičkog zahteva, manji kod neoštećene zgrade od globalnih driftova za scenarija oštećenja zgrade. Međutim, globalni driftovi za maksimalno realizovan nivo pomeranja (kolapsno stanje) mogu biti veći kod neoštećene zgrade, u odnosu na globalne driftove za scenarija oštećenja zgrade. Ovo je posledica toga što prilikom određenih scenarija oštećenja zgrade kolaps nastupa znatno ranije, nego što je to slučaj kod neoštećene zgrade, pa i nije moguće realizovati veći nivo pomeranja. Na taj način, stiče se utisak da je kod određenih scenarija oštećenja zgrade realizovan manji nivo povredljivosti, nego što je to slučaj kod neoštećene zgrade. U tom smislu, potrebno je pro-analizirati kolika su maksimalna realizovanja pomeranja i nivoi iniciranja kolapsa zgrade. S druge strane, međuspratni driftovi pri nivou ciljnog pomeranja 3D modela okvirne zgrade, određeni za isti nivo seizmičkog zahteva, mogu pokazati koliki je stepen povredljivosti oštećene zgrade, u odnosu na neoštećenu zgradu. U ovom slučaju, utvrđeno je da su međuspratni driftovi gotovo svi niži kod neoštećene zgrade, dok su kod određenih scenarija oštećene zgrade razvijani veći međuspratni driftovi čak i kod viših spratova koji nisu bili direktno oštećeni. To znači da se inicijalno oštećenje usled incidentnog dejstva povećalo pri dodatnom seizmičkom dejstvu. Međuspratni driftovi za maksimalno

5 CONCLUSION

Based on the developed methodology and non-linear numerical analysis of the 3D building model conducted, it has been concluded that global drifts at the level of target displacement obtained for the same level of seismic demand are lower in the undamaged building than global drifts in damaged-building scenarios. However, global drifts for the maximum realized displacement (collapse state) may be higher in the undamaged building than global drifts in the damaged-building scenarios. This is due to the fact that in certain damaged-building scenarios the collapse appears much earlier than it is the case with the undamaged building, so higher levels of displacement cannot be realized. Thus, one can get the impression that in certain damaged-building scenarios a lower level of vulnerability has been realized in comparison with the undamaged building. Therefore, it is necessary to identify the maximum realized displacement and the building's collapse initiation level. However, inter-storey drifts at the target displacement level of the 3D frame building model, determined for the same level of seismic demand, can indicate the degree of vulnerability of the damaged building compared to the undamaged building. In this case, almost all inter-storey drifts found in undamaged buildings were lower, while in some damaged-building scenarios higher inter-storey drifts were developed even in higher stories that were indirectly damaged. This means that the initial damage induced by accidental action has increased with the

realizovan nivo pomeranja (kolapsno stanje) neoštećene zgrade mogu biti veći nego kod oštećene zgrade, ali njih treba razmatrati u kontekstu s globalnim driftovima. U ovom slučaju, određivani su međuspratni driftovi za različite vrednosti globalnih driftova, a s obzirom na to što su kod skoro svih scenarija oštećenja zgrade realizovane znatno manje vrednosti globalnih driftova, moglo se i očekivati da će njihovi odgovarajući međuspratni driftovi biti manji. Međutim, kod viših spratova, oni su i za znatno manje vrednosti globalnih driftova veći nego u slučaju neoštećene zgrade.

Na osnovu definisanog i analiziranog koeficijenta oštećenja zgrade, može se pouzdano i veoma brzo odrediti stepen oštećenja sistema u kapacitativnom domenu. Potrebno je poznavati samo četiri parametra (inicijalno stanje, granica tečenja, nivo ojačanja/omekšanja i nivo maksimalnog pomeranja), kako bi se modeli originalnih *pushover* krivih veoma efikasno i tačno aproksimirali kroz interpolaciju trilinearnim splajnom. Generalno, može se zaključiti da - ukoliko je realizovan kolaps stubova prizemlja, a koji su neposredno jedan uz drugi - tada se može očekivati značajan stepen oštećenja zgrade. U ovom slučaju i kolaps manjeg broja stubova može predstavljati kritičniju situaciju u odnosu na neki drugi raspored većeg broja stubova. Ukoliko je realizovan kolaps stubova koji nisu na bliskoj udaljenosti, tada je i stepen oštećenja niži u odnosu na prethodno izveden stav. S druge strane, svaki model zgrade je poseban problem, pa detaljnija generalizacija nije ni moguća, jer se zahteva multiparametarski pristup u rešavanju ovakvih složenih problema, kao što je prikazano metodologijom razvijenom u ovom istraživanju.

additional seismic action. Inter-storey drifts for the maximum realized displacement (collapse state) of the undamaged building can be higher than those of the damaged building, but they should be considered in context with global drifts. In this case, inter-storey drifts were determined for various global drift values, as in almost all damage scenarios significantly lower global drift values were realized, which could have been expected provided that their corresponding inter-storey drifts were lower. However, at higher stories they were higher for even much lower global drift values than in the undamaged building.

Based on the defined and analyzed damage coefficient, the degree of damage to the system in the capacitive domain can be reliably and quickly identified. It requires only four parameters (the initial state, the yielding state, the level of hardening/softening and the level of maximum displacement) in order to approximate the models of original pushover curves very efficiently and accurately using tri-linear spline interpolation. Generally, it can be concluded that with the collapse of adjacent ground-floor columns, a significant degree of damage to the building can be expected. Thus, the collapse of few columns can lead to critical situation, as compared to some other arrangement with larger number of columns. With the collapse of columns that are not in the near distance, the degree of damage is also lower than in the above case. However, each building model makes an individual problem, which disables further generalization since solving such a complex problem requires the multi-parameter approach, as shown by the methodology developed in this research.

Zahvalnost

Prikazano istraživanje podržalo je Ministarstvo prosvete, nauke i tehnološkog razvoja Republike Srbije (Projekat br. TR 36043).

Acknowledgement

The presented work has been supported by The Ministry of Education and Science of the Republic of Serbia (Project No. TR 36043).

6 LITERATURA REFERENCES

[1] Adam C., Jager C.: *Dynamic Instabilities of Simple Inelastic Structures Subjected to Earthquake Excitation*, Advanced Dynamics and Model-Based Control of Structures and Machines, Springer, pp. 11-18, 2012.

[2] Adam C., Jager C.: *Seismic Induced Global Collapse of Non-deteriorating Frame Structures*, M. Papadrakakis et al. (eds.): Computational Methods in Earthquake Engineering, Springer, pp. 21-40, 2012.

[3] ATC 40, *Seismic Evaluation and Retrofit of Concrete Buildings*, Vol. 1, Applied Technology Council, Redwood City, USA, 1996.

[4] Bradley B., Dhakal R., Mander J.: *Modeling and Analysis of Multi-Storey Buildings Designed to Principles of Ductility and Damage Avoidance*, The 10th East Asia and Pacific Conference on Structural Engineering and Construction, Bangkok, Thailand, pp. 1-6, 2006.

[5] Chung Y., Meyer C., Shinozuka M.: *Seismic Damage Assessment of RC Members*, Report NCEER-87-0022, National Center for Earthquake Engineering Research, State University of New York at Buffalo, 1987.

[6] Ćosić M., Brčić S.: Metodologija pripreme i obrade akcelerograma za linearne i nelinearne seizmičke analize konstrukcija, Časopis Izgradnja, Vol. 66, No. 11-12, str. 511-526, 2012.

[7] DiPasquale E., Cakmak A.: Detection and Assessment of Seismic Structural Damage, Report NCEER-87-0015, National Center for Earthquake Engineering Research, State University of New York at Buffalo, 1987.

[8] EN 1992, Design of Concrete Structures - Part 1-1: General Rules and Rules for Buildings, European Committee for Standardization, Belgium, 2003.

[9] EN 1998, Design of Structures for Earthquake Resistance - Part 1: General Rules, Seismic Actions and Rules for Buildings, European Committee for Standardization, Belgium, 2004.

[10] Fahjan Y., Ozdemir Z., Keypour H.: Procedures for Real Earthquake Time Histories Scaling and Application to Fit Iranian Design Spectra, The 5th Iranian Conference on Seismology and Earthquake Engineering, Paper No. 164, pp. 1-8, Iran, Tehran, 2007.
[11] FEMA 273, *NEHRP Guidelines for the Seismic Rehabilitation of the Buildings*, Building Seismic Safety Council, Applied Technology Council, Federal Emergency Management Agency, Washington D. C., USA, 1997.
[12] FEMA 274, *NEHRP Commentary on the Guidelines for the Seismic Rehabilitation of the Buildings*, Building Seismic Safety Council, Applied Technology Council, Federal Emergency Management Agency, Washington D. C., USA, 1997.
[13] FEMA 356, *Pre-Standard and Commentary for the Seismic Rehabilitation of Buildings*, American Society of Civil Engineers, Federal Emergency Management Agency, Washington D. C., USA, 2000.
[14] Folić R., Ćosić M.: *Vulnerability of Damaged Structures: The Concept of the Scenario of Related Non-Linear Analyses*, International Conference on Civil Engineering Design and Construction (Science and Practice), pp. 14-26, Varna, Bulgaria, 2014.
[15] Ghobarah A., Abou-Elfath H., Biddah A.: *Response-Based Damage Assessment of Structures*, Earthquake Engineering and Structural Dynamics, Vol. 28, Iss. 1, pp. 79-104, 1999.
[16] Goulet C., Haselton C., Mitrani-Reiser J., Beck J., Deierlein G., Porter K., Stewart J.: *Evaluation of the Seismic Performance of a Code-Conforming Reinforced-Concrete Frame Building: From Seismic Hazard to Collapse Safety and Economic Losses*, Earthquake Engineering and Structural Dynamics, Vol. 36, Iss. 13, 2007.
[17] Haselton C., Liel A., Deierlein G., Brian D., Chou J.: *Seismic Collapse Safety of Reinforced Concrete Buildings. I: Assessment of Ductile Moment Frames*, Journal of Structural Engineering, Vol. 137, Iss. 4, pp. 481-491, 2011.
[18] http://www.isesd.hi.is/ESD_Local/frameset.htm
[19] Jeong S., Elnashai A.: *Analytical and Experimental Seismic Assessment of Irregular RC Buildings*, The 13th World Conference on Earthquake Engineering, Paper No. 113, Vancouver, Canada, pp. 1-15, 2004.
[20] Ladjinovic Dj., Folic R.: *Application of Improved Damage Index for Designing od Earthquake Resistant Structures*, The 13th World Conference on Earthquake Engineering, Paper No. 2135, Vancouver, Canada, pp. 1-15, 2004.
[21] Liel A., Haselton C., Deierlein G.: Seismic Collapse Safety of Reinforced Concrete Buildings. II: Comparative Assessment of Nonductile and Ductile Moment Frames, Journal of Structural Engineering, Vol. 137, Iss. 4, pp. 492-502, 2011.
[22] Lieping Y., Zhe Q.: Failure Mechanism and Its Control of Building Structures Under Earthquakes Based on Structural System Concept, Journal of Earthquake and Tsunami, Vol. 3, Iss. 4, pp. 249-259, 2009.
[23] Liolios A., Hatzigeorgiou G., Liolios A.: Efekat višestrukih zemljotresa na seizmički odgovor konstrukcije, Građevinski materijali i konstrukcije, Vol. 55, Iss. 4, pp. 3-14, 2012.
[24] Loh C-H., Chao A-H.: The Use of Damage Function in Performance-Based Seismic Design of Structures, The 13th World Conference on Earthquake Engineering, Paper No. 3257, Vancouver, Canada, pp. 1-15, 2004.
[25] Maeda M., Nakano Y., Lee K.: Post-Earthquake Damage Evaluation for R/C Buildings Based on Residual Seismic Capacity, The 13th World Conference on Earthquake Engineering, Paper No. 1179, Vancouver, Canada, pp. 1-15, 2004.
[26] Manafpour A.: A Damage-Controlled Force-Based Seismic Design Method for RC Frames, The 13th World Conference on Earthquake Engineering, Paper No. 2670, Vancouver, Canada, pp. 1-22, 2004.
[27] Nakano Y, Maeda M, Kuramoto H, Murakami M.: Guideline for Post-Earthquake Damage Evaluation and Rehabilitation of RC Buildings in Japan, The 13th World Conference on Earthquake Engineering, Paper No. 124, Vancouver, Canada, 2004.
[28] Park Y., Ang A., Wen Y.: Seismic Damage Analysis of Reinforced Concrete Buildings, Journal of Structural Engineering, Vol. 111, Iss. 4, pp. 740-757, 1985.
[29] Park Y., Ang A., Wen Y.: Damage-Limiting Aseismic Design of Buildings, Earthquake Spectra, Vol. 3, Iss.. 1, pp. 1-26, 1987.
[30] Roufaiel M., Meyer C.: Reliability of Concrete Frames Damaged by Earthquakes, Journal of Structural Engineering, Vol. 113, Iss. 3, pp. 445-457, 1987.
[31] Takada T., Nakano T.: Seismic Load Effect Directly Linked to Specified Collapse Mechanisms in Ultimate Limit State Design, The 12th World Conference on Earthquake Engineering, Paper No. 2560, Auckland, New Zealand, pp. 1-9, 2000.
[32] Vamvatsikos D., Cornell A.: Seismic Performance, Capacity and Reliability of Structures as Seen Through Incremental Dynamic Analysis, The John A. Blume Earthquake Engineering Center, Report No. 151, USA, 152p, 2005.
[33] Williams M., Sexsmith R.: Seismic Damage Indices for Concrete Structures: A State-of-the-Art Review, Earthquake Spectra, Vol 11, Iss. 2, pp. 319-349, 1995.

REZIME

ANALIZA PERFORMANSI OŠTEĆENIH OBJEKATA, PRIMENOM SCENARIJA POVEZANIH NELINEARNIH ANALIZA I KOEFICIJENTA OŠTEĆENJA

Mladen ĆOSIĆ
Radomir FOLIĆ

U radu je razvijena i prikazana metodologija za analizu oštećenja objekata koji su izloženi incidentnom i seizmičkom dejstvu. Procedura se bazira na nelinearnim numeričkim analizama, uvažavajući principe projektovanja konstrukcija prema seizmičkim performansama (PBSD). Matrica krutosti za uticaje vertikalnog dejstva koristi se kao inicijalna matrica krutosti prilikom nelinearne analize kojom se simulira kolaps pojedinačnih stubova prizemlja, formirajući nekoliko mogućih scenarija. Matrica krutosti na kraju analize, kojom se simulira kolaps pojedinačnih stubova, koristi se kao inicijalna matrica krutosti prilikom nelinearne statičke *pushover* analize (NSPA) za bidirekciono seizmičko dejstvo (X i Y pravac). Analize ciljnog pomeranja sprovedene su prema metodi spektra kapaciteta (CSM). Procena stanja zgrade je sprovedena na osnovu proračunatih globalnih i međuspratnih driftova i razvijenog koeficijenta oštećenja. Razmatranje stanja oštećenja zgrade utvrđeno je integralnim pistupom i preko globalnih i preko međuspratnih driftova, tako da se - u zavisnosti od nivoa pomeranja za koji se driftovi određuju - dobija pouzdaniji odgovor. Primenom koeficijenta oštećenja može se dobiti veoma brz, pouzdan i dovoljno precizan odgovor kada je reč o nivou oštećenja kompletne zgrade u kapacitativnom domenu, od elastičnog, preko nelinearnog, pa sve do stanja kolapsa.

Ključne reči: nelinearna analiza, scenario, incidentno i seizmičko dejstvo, koeficijent oštećenja

SUMMARY

PERFORMANCE ANALYSIS OF DAMAGED BUILDINGS APPLYING SCENARIO OF RELATED NON-LINEAR ANALYSES AND DAMAGE COEFFICIENT

Mladen COSIC
Radomir FOLIC

The paper deals with methodology developed and presented for analyzing the damage on structures exposed to accidental and seismic actions. The procedure is based on non-linear numerical analysis, taking into account the principles of *Performance-Based Seismic Design* (PBSD). The stiffness matrix of the effects of vertical action is used as the initial stiffness matrix in non-linear analysis which simulates the collapse of individual ground-floor columns, forming thereby a number of possible scenarios. By the end of the analysis that simulates the collapse of individual columns, the stiffness matrix is used as the initial stiffness matrix for *Non-linear Static Pushover Analysis* (NSPA) of bi-directional seismic action (X and Y directions). Target displacement analyses were conducted using the *Capacity Spectrum Method* (CSM). The structure's conditions/state was assessed based on the calculated global and inter-storey drifts and the damage coefficient developed. The damage level to the building was established using an integrated approach based on global and inter-storey drifts, so that, depending on the level of displacements for which the drifts are identified, a more reliable answer can be obtained. Applying the damage coefficient, a prompt, reliable and accurate indication can be obtained on the damage level to the entire structure in the capacitive domain, from elastic and non-linear to collapse state.

Keywords: non-linear analysis, scenario, accidental and seismic action, damage coefficient